Inorganic Chemistry

Crystal Structure Solid-State Cross Polarization Magic Angle Spinning ^{13}C NMR Correlation in Luminescent d^{10} Metal-Organic Frameworks Constructed with the 1,2-Bis(1,2,4-triazol-4-yl)ethane Ligand

Hesham A. Habib,[†] Anke Hoffmann,[*,‡] Henning A. Höppe,[†] Gunther Steinfeld,[†] and Christoph Janiak[*,†]

Institut für Anorganische und Analytische Chemie, Universität Freiburg, Albertstr. 21, D-79104 Freiburg, Germany, and Institut für Makromolekulare Chemie, Universität Freiburg, Stefan-Meier-Str. 31, D-79104 Freiburg, Germany
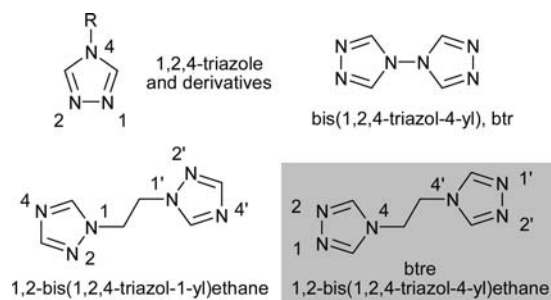
Hydrothermal reactions of 1,2-bis(1,2,4-triazol-4-yl)ethane (btre) with copper(II), zinc(II), and cadmium(II) salts have yielded the dinuclear complexes [Zn$_2$Cl$_4$(μ_2-btre)$_2$] (**1**) and [Zn$_2$Br$_4$(μ_2-btre)$_2$] (**2**), the one-dimensional coordination polymer $^1_\infty$[Zn(NCS)$_2$(μ_2-btre)] (**3**), the two-dimensional networks $^2_\infty$[Cu$_2$(μ_2-Cl)$_2$(μ_4-btre)] (**4**), $^2_\infty$[Cu$_2$(μ_2-Br)$_2$(μ_4-btre)] (**5**), and $^2_\infty$\{[Cd$_6$(μ_3-OH)$_2$(μ_3-SO$_4$)$_4$(μ_4-btre)$_3$(H$_2$O)$_6$](SO$_4$) · ~6H$_2$O\} (**6**), and the three-dimensional frameworks $^3_\infty$\{[Cu(μ_4-btre)]ClO$_4$ · ~0.25H$_2$O\} (**7**), $^3_\infty$\{[Zn(μ_4-btre)(μ_2-btre)](ClO$_4$)$_2$\} (**8**), $^3_\infty$\{[Cd(μ_4-btre)(μ_2-btre)](ClO$_4$)$_2$\} (**9**), and $^3_\infty$[Cu$_2$(μ_2-CN)$_2$(μ_4-btre)] (**10**, 2-fold 3D interpenetrated framework). The copper-containing products **4**, **5**, **7**, and **10** contain the metal in the +1 oxidation state, from a simultaneous redox and self-assembly reaction of the Cu(II) starting materials. The cyanide-containing framework **10** has captured the CN$^-$ ions from the oxidative btre decomposition. The perchlorate frameworks **7**, **8**, or **9** react in an aqueous NH$_4^+$PF$_6^-$ solution with formation of the related PF$_6^-$-containing frameworks. The differences in the metal-btre bridging mode (μ_2-κN1:N1′, μ_2-κN1:N2 or μ_4-κN1:N2:N1′:N2′) and the btre ligand symmetry can be correlated with different signal patterns in the ^{13}C cross polarization magic angle spinning (CPMAS) NMR spectra. Compounds **2**, **4**, **5** and **7** to **10** exhibit fluorescence at 403−481 nm upon excitation at 270−373 nm which is not seen in the free btre ligand.

Introduction

Coordination polymers, metal coordination networks, or metal-organic frameworks (MOFs) are of contemporary interest because of their structural topologies and potential applications in the areas of catalysis, adsorption, luminescence, nonlinear optics, magnetism, and ion exchange.[1−4] Coordination compounds containing derivatives of 1,2,4-triazole have been of increasing interest during the past decade.[1] The 1,2,4-triazole ligand and its 4-substituted derivatives (Scheme 1) can be used to obtain a wide variety of polynuclear molecules[5] and linear coordination polymers based on its bridging function, for example, with Cu^{2+},[6] Zn^{2+},[7] and Cd^{2+}.[8] The N1:N2-bridging mode of 1,2,4-triazole

* To whom correspondence should be addressed. E-mail: anke.hoffmann@makro.uni-freiburg.de (A.H.), janiak@uni-freiburg.de (C.J.). Fax: +49 761 2036306 (A.H.), 49 761 2036147 (C.J.). Phone: +49 761 203631 (A.H.), 49 761 2036127 (C.J.).
† Institut für Anorganische und Analytische Chemie.
‡ Institut für Makromolekulare Chemie.

Scheme 1. Common 1,2,4-Triazole Derivatives for the Construction of Metal Coordination Networks^a

^{a} The gray underlined ligand btre is synthetically used in this work.

or triazolate constitutes a short ligand bridge between metal atoms which is a prerequisite for stronger magnetic coupling between paramagnetic metal centers.[1] Surprisingly, with the related 4,4′-bis(1,2,4-triazol-4-yl) ligand (abbreviated as btr, Scheme 1) this N1:N2 bridging coordination mode has only been observed recently with Cu(II).[9] Typically the btr ligand

links transition metal(II) ions using only one nitrogen atom from each 1,2,4-triazole ring resulting in one-,[10,11] two-, and three-dimensional (1D, 2D, 3D) networks.[12−14] When spacers, like methylene groups, are introduced between the two 1,2,4-triazole rings, the resulting ligand acquires more flexibility. Therefore, we selected 1,2-bis(1,2,4-triazol-4-yl)ethane (abbreviated as btre).[15] This btre ligand must not be mistaken with the more widely employed 1,2-bis(1,2,4-triazol-*1*-yl)ethane[16] and other ∼alkane ligands (Scheme 1).[17] These related 1,2-bis(1,2,4-triazol-*1*-yl) ligands do only bridge between two metal atoms in a $\kappa N4:N4'$ mode. Hence, they cannot bring two metal atoms closely together as the btre ligand can through its $\kappa N1$:

*N*2 bridge. At the same time, the btre ligand has been scarcely used in metal-complex or MOF synthesis. A CSD search[18] gave $^{2}_{\infty}\{M(NCS)_{2}(\mu_{2}\text{-btre-}\kappa N1{:}N1')_{2}(NCS)_{2}\}$ (M = Fe, Co)[19] and $^{3}_{\infty}\{[Cu_{3}(\mu_{4}\text{-btre-}\kappa N1{:}N2{:}N1'{:}N2')_{2}(\mu_{3}\text{-btre-}\kappa N1{:}N2{:}N1')_{4}(H_{2}O)_{2}]_{2}(ClO_{4})_{12}\cdot 2H_{2}O\}$[20] as the only examples. We have recently added mixed-ligand 1D to 3D coordination networks[21] of btre with benzene-1,3,5-tricarboxylate or benzene-1,4- and -1,3-dicarboxylate and Ni(II), Cu(II), Zn(II) or Cd(II) as metal atoms which feature solid-state crystal-

(1) Reviews about coordination polymers/MOFs: Application oriented properties Janiak, C. *Dalton Trans.* **2003**, 2781–2804. Mueller, U.; Schubert, M.; Teich, F.; Puetter, H.; Schierle-Arndt, K.; Pastré, J. *J. Mater. Chem.* **2006**, *16*, 626–636. Lin, X.; Jia, J.; Hubberstey, P.; Schröder, M.; Champness, N. R. *CrystEngComm* **2007**, *9*, 438–448. Collins, D. J.; Zhou, H.-C. *J. Mater. Chem.* **2007**, *17*, 3154–3160. f-Elements: Cahill, C. L.; de Lill, D. T.; Frisch, M. *CrystEngComm* **2007**, *9*, 15–26. Silver(I): Chen, C.-L.; Kang, B.-S.; Su, C.-Y. *Aust. J. Chem.* **2006**, *59*, 3–18. Imidazolate-, triazolate-ligands: Zhang, J.-P.; Chen, X.-M. *Chem. Commun.* **2006**, 1689–1699. Interpenetration: Blatov, V. A.; Carlucci, L.; Ciani, G.; Proserpio, D. M. *CrystEngComm* **2004**, *6*, 377–395. Carlucci, L.; Ciani, G.; Proserpio, D. *Coord. Chem. Rev.* **2003**, *246*, 247–289. Luminescence: Zheng, S.-L.; Chen, X.-M. *Aust. J. Chem.* **2004**, *57*, 703–712. Magnetism: Maspoch, D.; Ruiz-Molina, D.; Veciana, J. *Chem. Soc. Rev.* **2007**, *36*, 770–818. O- and N-donors: Robin, A. Y.; Fromm, K. M. *Coord. Chem. Rev.* **2006**, *250*, 2127–2157. Porosity: Férey, G. *Chem. Soc. Rev.* **2008**, *37*, 191–214. Bureekaew, S.; Shimomura, S.; Kitagawa, S. *Sci. Technol. Adv. Mat.* **2008**, *9*, Art. No. 014108. Maji, T. K.; Kitagawa, S. *Pure Appl. Chem.* **2007**, *79*, 2155–2177. Kitagawa, S.; Matsuda, R. *Coord. Chem. Rev.* **2007**, *251*, 2490–2509. Kitagawa, S.; Noro, S.-I.; Nakamura, T. *Chem. Commun.* **2006**, 701–707.

(2) Recent examples on magnetism in coordination polymers/metal-organic frameworks: (a) Drabent, K.; Ciunik, Z.; Ozarowski, A. *Inorg. Chem.* **2008**, *47*, 3358–3365. (b) Branzea, D. G.; Sorace, L.; Maxim, C.; Andruh, M.; Caneschi, A. *Inorg. Chem.* **2008**, *47*, 6590–6592. (c) Zheng, Y.-Z.; Xue, W.; Tong, M.-L.; Chen, X.-M.; Grandjean, F.; Long, G. J. *Inorg. Chem.* **2008**, *47*, 4077–4087. (d) Agustí, G.; Muñoz, M. C.; Gaspar, A. B.; Real, J. A. *Inorg. Chem.* **2008**, *47*, 2552–2561. (e) Wang, X.-Y.; Sevov, S. C. *Inorg. Chem.* **2008**, *47*, 1037–1043. Sessoli, R. *Inorg. Chim. Acta* **2008**, *361*, 3356–3364. (f) Rentschler, E.; von Malotki, C. *Inorg. Chim. Acta* **2008**, *361*, 3646–3653. (g) Mole, R. A.; Cottrell, S. P.; Stride, J. A.; Wood, P. T. *Inorg. Chim. Acta* **2008**, *361*, 3718–3722. (h) Abu-Youssef, M. A. M.; Mautner, F. A.; Vicente, R. *Inorg. Chim. Acta* **2008**, *361*, 895–2900. (i) Ray, A.; Chakraborty, J.; Samanta, B.; Thakurta, S.; Marschner, C.; El Fallah, M. S.; Mitra, S. *Inorg. Chim. Acta* **2008**, *361*, 1850–1860. (h) Habib, H. A.; Sanchiz, J.; Janiak, C. *Dalton Trans.* **2008**, 4877–4884. (j) Matouzenko, G. S.; Perrin, M.; Le Guennic, B.; Genre, C.; Molnar, G.; Bousseksou, A.; Borshch, S. A. *Dalton Trans.* **2007**, 934–942. (k) Chakraborty, J.; Nandi, M.; Mayer-Figge, H.; Sheldrick, W. S.; Sorace, L.; Bhaumik, A.; Banerjee, P. *Eur. J. Inorg. Chem.* **2007**, 5033–5044. (m) Seredyuk, M.; Gaspar, A. B.; Munoz, M. C.; Verdaguer, M.; Villain, F.; Gütlich, P. *Eur. J. Inorg. Chem.* **2007**, 4481–4491.

(3) Recent examples on luminescence in coordination polymers/metal-organic frameworks: (a) Daiguebonne, C.; Kerbellec, N.; Guillou, O.; Bünzli, J.-C.; Gumy, F.; Catala, L.; Mallah, T.; Audebrand, N.; Gérault, Y.; Bernot, K.; Calvez, G. *Inorg. Chem.* **2008**, *47*, 3700–3708. (b) Zhang, P.; Niu, Y.-Y.; Wu, B. L.; Zhang, H.-Y.; Niu, C.-Y.; Hou, H.-W. *Inorg. Chim. Acta* **2008**, *361*, 2609–2615. (c) Chelebaeva, E.; Larionova, J.; Guari, Y.; Sa Ferreira, R. A.; Carlos, L. D.; Almeida Paz, F. A.; Trifonov, A.; Guerin, C. *Inorg. Chem.* **2008**, *47*, 775–777. (d) Genuis, E. D.; Kelly, J. A.; Patel, M.; McDonald, R.; Ferguson, M. J.; Greidanus-Strom, G. *Inorg. Chem.* **2008**, *47*, 6184–6194. (e) Wang, Y.; Ding, B.; Cheng, P.; Liao, D.-Z.; Yan, S.-P. *Inorg. Chem.* **2007**, *46*, 2002–2010. (f) Fu, F.; Hu, S.; Wu, X. *Inorg. Chem.* **2007**, *46*, 9630–9640. (g) Ye, J.-W.; Wang, J.; Zhang, J.-Y.; Zhang, P.; Wang, Y. *CrystEngComm* **2007**, *9*, 515–523. (h) Chu, Q.; Kong, L.-Y.; Okamura, T.; Kawaguchi, H.; Meng, W.-L.; Sun, W.-Y.; Ueyama, N. *Z. Anorg. Allg. Chem.* **2007**, *633*, 326–331. (i) Girginova, P. I.; Paz, F. A.; Soares-Santos, P. C. R.; Ferreira, R. A. S.; Carlos, L. D.; Amaral, V. S.; Klinowski, J.; Nogueira, H. I. S.; Trindade, T. *Eur. J. Inorg. Chem.* **2007**, 4238–4246.

(4) Recent examples on structural work in coordination polymers/metal-organic framework: (a) Caskey, S. R.; Matzger, A. J. *Inorg. Chem.* **2008**, *47*, 7942–7944. (b) Zhao, N.; Bullinger, J. C.; Van Stipdonk, M. J.; Stern, C. L.; Eichhorn, D. M. *Inorg. Chem.* **2008**, *47*, 5945–5950. (c) Wang, X.; Bi, Y.; Chen, B.; Lin, H.; Liu, G. *Inorg. Chem.* **2008**, *47*, 2442–2448. (d) An, C. X.; Lu, Y. C.; Shang, Z. F.; Zhang, Z. H. *Inorg. Chim. Acta* **2008**, *361*, 2721–2730. (e) Wu, B.-L.; Zhang, P.; Niu, Y.-Y.; Zhang, H.-Y.; Li, Z.-J.; Hou, H.-W. *Inorg. Chim. Acta* **2008**, *361*, 2203–2209. (f) Wei, X. Y.; Di, Z.; Zhu, Q. L.; Huang, R. D. *Inorg. Chim. Acta* **2008**, *361*, 1819–1826. (g) Jia, D.; Zhu, A.; Deng, J.; Zhang, Y.; Dai, J. *Dalton Trans.* **2007**, 2083–2086. (h) Sato, N.; Nishikiori, S.-I. *Dalton Trans.* **2007**, 1115–1119. (i) Carballo, R.; Covelo, B.; Garcia-Martinez, E.; Lago, A. B.; Vázquez-López, E. M. *Z. Anorg. Allg. Chem.* **2007**, *633*, 780–782. (j) Knapp, W. R.; Thomas, J. G.; Martin, D. P.; Braverman, M. A.; Trovitch, R. J.; LaDuca, R. L. *Z. Anorg. Allg. Chem.* **2007**, *633*, 575–581. (k) Roth, A.; Buchholz, A.; Plass, W. *Z. Anorg. Allg. Chem.* **2007**, *633*, 383–392. (l) Cho, S.-H.; Gadzikwa, T.; Afshari, M.; Nguyen, S. T.; Hupp, J. *Eur. J. Inorg. Chem.* **2007**, 4863–4867. (m) He, C.; Zhao, Y.; Guo, D.; Lin, Z.; Duan, C. *Eur. J. Inorg. Chem.* **2007**, 3451–3463. (n) Beves, J. E.; Constable, E. C.; Housecroft, C. E.; Kepert, C. J.; Price, D. J. *CrystEngComm* **2007**, *9*, 456–459. (o) Thuéry, P. *CrystEngComm* **2007**, *9*, 460–462. (p) Gu, X.; Xue, D. *CrystEngComm* **2007**, *9*, 471–477. (q) Krishnan, S. M.; Patel, N. M.; Knapp, W. R.; Supkowski, R. M.; LaDuca, R. L. *CrystEngComm* **2007**, *9*, 503–514. (r) Mueller-Buschbaum, K.; Mokaddem, Y. *Z. Anorg. Allg. Chem.* **2007**, *633*, 521–523.

(5) (a) Vos, G.; de Kok, A. J.; Verschoor, G. C. *Z. Naturforsch.* **1981**, *B36*, 809. (b) Schmidbaur, H.; Mair, A.; Müller, G.; Lachmann, J.; Gamper, S. *Z. Naturforsch.* **1991**, *B46*, 912. (c) Castillo, O.; Garcia-Couceiro, U.; Luque, A.; Garcia-Teran, J. P.; Roman, P. *Acta Crystallogr.* **2004**, *E60*, m9. (d) Xuan-Wen, L. *Acta Crystallogr.* **2005**, *E61*, m1777. (e) Nockemann, P.; Schulz, F.; Naumann, D.; Meyer, G. *Z. Anorg. Allg. Chem.* **2005**, *631*, 649. (f) Ding, B.; Yi, L.; Wang, Y.; Cheng, P.; Liao, D.-Z.; Yan, S.-P.; Jiang, Z.-H.; Song, H.-B.; Wang, H.-G. *Dalton Trans.* **2006**, 665. (g) Liu, B.; Xu, L.; Guo, G.-C.; Huang, J.-S. *J. Mol. Struct.* **2006**, *825*, 79. (h) Aznar, E.; Ferrer, S.; Borras, J.; Lloret, F.; Liu-Gonzalez, M.; Rodriguez-Prieto, H.; Garcia-Granda, S. *Eur. J. Inorg. Chem.* **2006**, 5115.

(6) (a) Garcia, Y.; van Koningsbruggen, P. J.; Bravic, G.; Guionneau, P.; Chasseau, D.; Cascarano, G. L.; Moscovici, J.; Lambert, K.; Michalowicz, A.; Kahn, O. *Inorg. Chem.* **1997**, *36*, 6357. (b) Liu, J.-C.; Fu, D.-G.; Zhuang, J.-Z.; Duan, C.-Y.; You, X.-Z. *J. Chem. Soc., Dalton Trans.* **1999**, 2337. (c) Hagrman, P. J.; Bridges, C.; Greedan, J. E.; Zubieta, J. *J. Chem. Soc., Dalton Trans.* **1999**, 2901. (d) Drabent, K.; Ciunik, Z. *Chem. Commun.* **2001**, 1254. (e) Garcia, Y.; Moscovici, J.; Michalowicz, A.; Ksenofontov, V.; Levchenko, G.; Bravic, G.; Chasseau, D.; Gütlich, P. *Chem.−Eur. J.* **2002**, *8*, 4992. (f) Garcia, Y.; van Koningsbruggen, P. J.; Bravic, G.; Chasseau, D.; Kahn, O. *Eur. J. Inorg. Chem.* **2003**, 356. (g) Liu, B.; Guo, G.-C.; Huang, J.-S. *J. Solid State Chem.* **2006**, *179*, 3136. (h) Ding, B.; Huang, Y. Q.; Liu, Y. Y.; Shi, W.; Cheng, P. *Inorg. Chem. Commun.* **2007**, *10*, 7.

(7) Park, H.; Moureau, D. M.; Parise, J. B. *Chem. Mater.* **2006**, *18*, 525.

(8) (a) Yi, L.; Ding, B.; Zhao, B.; Cheng, P.; Liao, D.-Z.; Yan, S.-P.; Jiang, Z.-H. *Inorg. Chem.* **2004**, *43*, 33. (b) Huang, Y.-Q.; Ding, B.; Song, H.-B.; Zhao, B.; Ren, P.; Wang, H.-G.; Liao, D.-Z.; Yan, S.-P. *Chem. Commun.* **2006**, 4906.

(9) (a) Lysenko, A. B.; Govor, E. V.; Krautscheid, H.; Domasevitch, K. V. *Dalton Trans.* **2006**, 3772. (b) Lysenko, A. B.; Govor, E. V.; Domasevitch, K. V. *Inorg. Chim. Acta* **2007**, *360*, 55.

(10) [Mn(NCS)₂(μ-btr-κN1,N1′)(H₂O)₂]: Biagini-Cingi, M.; Manotti-Lanfredi, A. M.; Ugozzoli, F.; Haasnoot, J. G.; Reedijk, J. *Gazz. Chim. Ital.* **1994**, *124*, 509.

(11) {[Mn(NCS)(μ-btr-κN1,N1′)(btr-kN1)₂(H₂O)]NCS}: Zilverentant, C. L.; Driessen, W. L.; Haasnoot, J. G.; Kolnaar, J. J. A.; Reedijk, J. *Inorg. Chim. Acta* **1998**, *282*, 257.

(12) [Co(NCS)₂(μ-btr-κN1,N1′)₂]: Vreugdenhil, W.; Gorter, S.; Haasnoot, J. G.; Reedijk, J. *Polyhedron* **1985**, *4*, 1769.

Scheme 2. Schematic Metal-Ligand Connectivity in **1–10**[a]
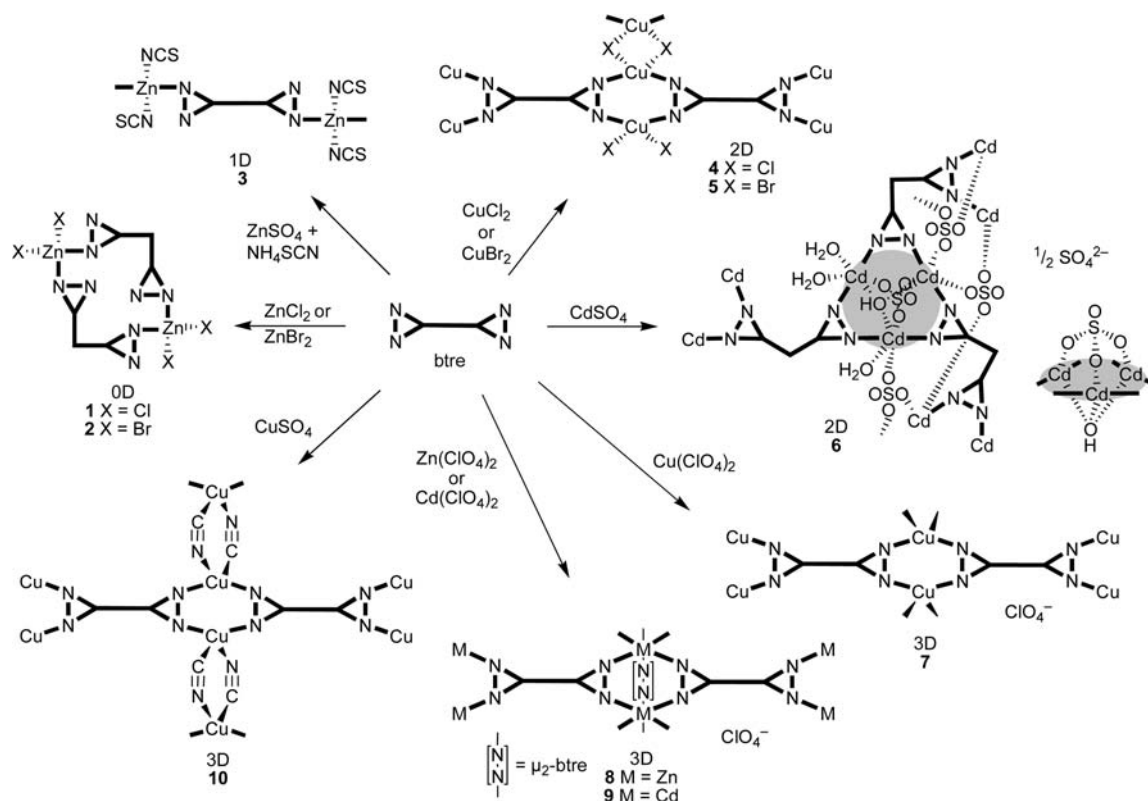
[a] The metal-btre bonds are depicted as bold lines.

to-crystal transitions upon drying (Ni, Zn), luminescence (Zn, Cd), or ferro- (Cu) and antiferromagnetic (Ni) coupling. The hitherto most often observed btre coordination mode is μ_4-btre-$\kappa N1{:}N2{:}N1'{:}N2'$ where the bis-triazole-type ligand bridges between four metal atoms occupying all of its sp^2-hybridized nitrogen atoms (cf. Scheme 2).[22]

In this work, we report the syntheses, structures, structure-Cross Polarization Magic Angle Spinning (CPMAS)-NMR correlations and luminescence of metal-btre complexes, coordination polymers, and networks with the d^{10} metal atoms Cu^+, Zn^{2+}, and Cd^{2+}.

Results and Discussion

Syntheses. Hydrothermal treatment of copper(II) chloride or bromide, zinc(II) chloride or bromide, zinc(II) sulfate in the presence of NH_4SCN, and cadmium(II) sulfate with 1,2-bis(1,2,4-triazol-4-yl)ethane (btre) yields the dinuclear complexes $[Zn_2Cl_4(\mu_2\text{-btre})_2]$ (**1**) and $[Zn_2Br_4(\mu_2\text{-btre})_2]$ (**2**), the 1D coordination polymer $^1_\infty[Zn(NCS)_2(\mu_2\text{-btre})]$ (**3**) and the 2D networks $^2_\infty[Cu_2(\mu_2\text{-Cl})_2(\mu_4\text{-btre})]$ (**4**), $^2_\infty[Cu_2(\mu_2\text{-Br})_2(\mu_4\text{-btre})]$ (**5**), and $^2_\infty\{[Cd_6(\mu_3\text{-OH})_2(\mu_3\text{-SO}_4)_4(\mu_4\text{-btre})_3\text{-}(H_2O)_6](SO_4)\cdot{\sim}6H_2O\}$ (**6**) (Scheme 2). For the synthesis of 3D metal-btre frameworks metal salts with less coordinating anions, that is, the perchlorates of copper(II), zinc(II), or cadmium(II) were reacted under hydrothermal conditions with btre to yield $^3_\infty\{[Cu(\mu_4\text{-btre})]ClO_4\cdot{\sim}0.25H_2O\}$ (**7**), $^3_\infty\{[Zn(\mu_4\text{-btre})(\mu_2\text{-btre})](ClO_4)_2\}$ (**8**), and $^3_\infty\{[Cd(\mu_4\text{-btre})(\mu_2\text{-btre})](ClO_4)_2\}$ (**9**). The product $^3_\infty[Cu_2(\mu_2\text{-CN})_2(\mu_4\text{-btre})]$ (**10**) is special as it originated from $CuSO_4$ and btre to contain cyanide bridges from the apparent btre decomposition (see below, Scheme 2).

(13) [Mn(μ-N₃-κN1,N3)₂(btr-kN1)₂]: Wang, X.-Y.; Wang, L.; Wang, Z.-M.; Su, G.; Gao, S. *Chem. Mater.* **2005**, *17*, 6369.

(14) [Fe(NCS)₂(μ-btr-κN1,N1′)₂]: Vreugdenhil, W.; van Diemen, J. H.; de Graaff, R. A. G.; Haasnoot, J. G.; Reedijk, J.; van der Kraan, A. M.; Kahn, O.; Zarembowitch, J. *Polyhedron* **1990**, *9*, 2971.

(15) Habib, H. A.; Janiak, C. *Acta Crystallogr.* **2008**, *E64*, o1199.

(16) (a) Zhu, X.; Zhang, Y.; Li, B.; Zhang, Y. *J. Coord. Chem.* **2006**, *59*, 513. (b) Zhu, X.; Li, B.; Zhou, J.; Li, B.; Zhang, Y. *Acta Crystallogr.* **2004**, *C60*, m191. (c) Zhou, J.; Zhu, X.; Zhang, Y.; Zhang, Y.; Li, B. *Inorg. Chem. Commun.* **2004**, *7*, 949. (d) Li, B.; Li, B.; Zhu, X.; Lu, X.; Zhang, Y. *J. Coord. Chem.* **2004**, *57*, 1361. (e) Li, B.; Zhu, X.; Zhou, J.; Peng, Y.; Zhang, Y. *Polyhedron* **2004**, *23*, 3133.

(17) (a) Tian, A.; Ying, J.; Peng, J.; Sha, J.; Han, Z.; Ma, J.; Su, Z.; Hu, N.; Jia, H. *Inorg. Chem.* **2008**, *47*, 3274. (b) Wang, X.-L.; Qin, C.; Wang, E.-B.; Su, Z.-M. *Chem.—Eur. J.* **2006**, *12*, 2680. (c) Wang, W.-B.; Wang, L.-Y.; Li, B.-L.; Zhang, Y. *Acta Crystallogr.* **2007**, *E63*, m2416. (d) Peng, Y.-F.; Ge, H.-Y.; Li, B.-Z.; Li, B.-L.; Zhang, Y. *Cryst. Growth Des.* **2006**, *6*, 994.

(18) Cambridge Structure Database search, CSD Version 5.28 (November 2006) with 2 updates (Januar 2007, May 2007).

(19) Garcia, Y.; Bravic, G.; Gieck, C.; Chasseau, D.; Tremel, W.; Gütlich, P. *Inorg. Chem.* **2005**, *44*, 9723.

(20) Garcia, Y.; van Koningsbruggen, P. J.; Kooijman, H.; Spek, A. L.; Haasnoot, J. G.; Kahn, O. *Eur. J. Inorg. Chem.* **2000**, 307.

(21) Recent examples for mixed-ligand coordination polymers: (a) Wisser, B.; Lu, Y.; Janiak, C. *Z. Anorg. Allg. Chem.* **2007**, *633*, 1189–1192. (b) Manna, S. C.; Okamoto, K.-I.; Zangrando, E.; Chaudhuri, N. R. *CrystEngComm* **2007**, *9*, 199–292. (c) Chen, Z.-F.; Zhang, S.-F.; Luo, H.-S.; Abrahams, B. F.; Liang, H. *CrystEngComm* **2007**, *9*, 27–29. (d) Pichon, A.; Fierro, C. M.; Nieuwenhuyzen, M.; James, S. *CrystEngComm* **2007**, *9*, 449–451. (e) Pasán, J.; Sanchiz, J.; Lloret, F.; Julve, M.; Ruiz-Pérez, C. *CrystEngComm* **2007**, *9*, 478–487. (f) Carballo, R.; Covelo, B.; Vázquez-López, E. M.; García-Martínez, E.; Castiñeiras, A.; Janiak, C. *Z. Anorg. Allg. Chem.* **2005**, *631*, 2006–2010.

(22) Habib, H. A.; Sanchiz, J.; Janiak, C. *Dalton Trans.* **2008**, 1734–1744.

Hydrothermal synthesis has been widely employed to construct assemblies of metal complexes in recent years. Noteworthy, all of the above copper-containing products **4**, **5**, **7**, and **10** contain the metal in the +1 oxidation state, from a simultaneous redox and self-assembly reaction of the Cu(II) starting materials. It is known that Cu^{2+} ions can be reduced to Cu^+ by N-, O-, and S-containing ligands, such as 4,4′-bipyridine, pyridine-4-thiol, quinoxaline, and pyridinedicarboxylate under hydrothermal conditions.[23−25] Also, under hydro(solvo)thermal conditions, the simultaneous redox and self-assembly reaction of Cu^{2+} with organonitrogen species was observed where the organonitrogen species behave not only as ligands but also as reducing agents toward Cu(II). This reduction then results in a decomposition of part of the organonitrogen species.[26−28] The product $^3_\infty[Cu_2(\mu_2\text{-}CN)_2(\mu_4\text{-btre})]$ (**10**) captures the cyanide ions from such a btre decompositon under hydrothermal conditions in the presence of Cu(II).

The vibrational modes for the triazole rings in the fingerprint region confirm the presence of btre ligand in the compounds **1−10**. A strong band at 2069 cm^{-1} in the IR spectrum of **3** indicates the metal-isothiocyanate, M−NCS coordination. The perchlorate anion was observed as a strong band in the spectra of **7**, **8**, and **9** at 1071, 1076, and 1073 cm^{-1} (cf. Figures S1−S3, Supporting Information,), respectively.[29,30] Sulfate bands in the IR spectrum of **6** occur at 1270 cm^{-1} (terminal S−O) and at 1112, 1062, and 960 cm^{-1} (coordinated S−O) which agree with the tridentate SO_4-coordination to three Cd atoms.[31,32] The IR spectrum of **10** showed a strong peak at 2094 cm^{-1} which is assigned to the bridging cyanide groups.[33,34] The M−N, M−Cl, and M−Br vibration bands are observed in the range of 632−405 cm^{-1}.

To check the possibility of ion exchange, freshly prepared crystals of the perchlorate containing 3D-frameworks **7**, **8**, or **9** were immersed in an aqueous solution of NH_4PF_6 (3 mol/L) for 24 h, then filtered off, washed thoroughly with water, and air-dried to give crystalline materials **7′**, **8′**, or **9′**, respectively. The infrared spectra of **7′−9′** show the disappearance or absence of the intense ClO_4^- peaks (1071−1076 cm^{-1}, see above) and the appearance of equally intense PF_6^- peaks (822−823 and 554−556 cm^{-1}) (Figures S1−S3, Supporting Information).[31,32] Also, the ^{31}P and ^{19}F NMR of **7′**, **8′**, and **9′** (dissolved in DMSO-d_6) show signals in the range −143 to −145 ppm for ^{31}P and in the range of −71 to −75 ppm for ^{19}F indicating the presence of the PF_6^-

anion in the structures. The products **7′**, **8′**, and **9′** are still in a crystalline state and isostructural for **7′** and **8′** to their starting materials as evidenced by their very similar X-ray powder diffractograms, although the crystal transparency was lost (Figures S4−S6, Supporting Information). However, during the ion-exchange reaction, the crystals do not retain their shape but disappear and reform (see sequence of photographs in Figure S7, Supporting Information). Thus, the ClO_4^--containing 3D-frameworks **7−9** do not undergo an ion-exchange in a (topotactic) solid-state crystal-to-crystal transformation but recrystallize to the apparently less soluble PF_6^--containing frameworks.

Thermal Stability. All of the isolated compounds are stable up to 270−300 °C without decomposition, except **6**. Compounds **1**, **2**, **4**, and **5** show a rather steady weight loss starting at ∼300 °C and continuing to over 600 °C because of the removal of the btre ligands (see Figures S8−S11, Supporting Information). A continuous weight loss for **3** from 275 to 600 °C is assigned to the removal of the organic ligand (obs. 45.4, calcd 47.5%, see Figure S12, Supporting Information) with 54.4% of the original mass retained as $Zn(NCS)_2$ (calcd 52.5%). Compound **6** shows the first weight loss in the temperature range 70−130 °C which corresponds to the removal of the crystal water molecules (obs. 4.2, calcd 5.7% for six or 3.9% for four remaining crystal water in the air-dried sample). From 150 to 280 °C a second weight loss of 6.1% occurs which is assigned to the six coordinated aqua ligands (calcd 5.7). A continuing weight loss from 290 to over 600 °C includes the loss of the btre ligands (Figure S13, Supporting Information). Noteworthy, in **10** only about half of the btre ligand is lost from 320−560 °C (obs. 24.0, calcd 47.8% btre fraction in **10**, Figure S14, Supporting Information). At 650 °C the remaining mass of 73.3% for **10** probably still includes some of the btre ligand. The perchlorate compounds **7**, **8**, and **9** explode at 310 °C under the thermogravimetric conditions.

Crystal Structures. The representative nature of the single crystals investigated by X-ray diffactometry was in all cases verified by positively matching the measured X-ray powder diffractogram of a larger crystal selection with the diffractogram simulated from the data of the single-crystal X-ray refinement (see Figures S15−S23, Supporting Information).

$[Zn_2Cl_4(\mu_2\text{-btre})_2]$ 1 and $[Zn_2Br_4(\mu_2\text{-btre})_2]$ 2. The isomorphous zinc compounds **1** and **2** feature a dinuclear complex molecule in which two cis-bent btre ligands bridge between two zinc atoms. Only one nitrogen atom on each triazole ring is used for metal coordination in a μ_2-btre-$\kappa N1$:$N1'$ mode, different from the μ_4-btre-$\kappa N1$:$N2$:$N1'$:$N2'$ mode in the complexes **4−10** (see below). The tetrahedral coordination sphere of each Zn atom is concluded by two halide ligands (Figure 1). The intermolecular packing in **1** and **2** is

(23) Yaghi, O. M.; Li, H. *J. Am. Chem. Soc.* **1995**, *117*, 10401.
(24) Wu, C. D.; Lu, C. Z.; Zhuang, H. H.; Huang, J. S. *Inorg. Chem.* **2002**, *41*, 5636.
(25) Lu, J. Y.; Babb, A. M. *Inorg. Chem.* **2002**, *41*, 1339.
(26) Cheng, J. K.; Yao, Y. G.; Zhang, J.; Li, Z. J.; Cai, Z. W.; Zhang, X. Y.; Chen, Z. N.; Chen, Y. B.; Kang, Y.; Qin, Y. Y.; Wen, Y. H. *J. Am. Chem. Soc.* **2004**, *126*, 7796.
(27) Kang, Y.; Yao, Y. G.; Qin, Y. Y.; Zhang, J.; Chen, Y. B.; Li, Z. J.; Wen, Y. H.; Cheng, J. K.; Hu, R. F. *Chem. Commun.* **2004**, 1046.
(28) Wen, Y. H.; Cheng, J. K.; Zhang, J.; Li, Z. J.; Kang, Y.; Yao, Y. G. *Inorg. Chem. Commun.* **2004**, *7*, 1120.
(29) Yaghi, O. M.; Li, H.; Groy, T. L. *Inorg. Chem.* **1997**, *36*, 4292.
(30) Min, K. S.; Suh, M. P. *J. Am. Chem. Soc.* **2000**, *122*, 6834–6840.
(31) Clegg, W.; Errington, R. J.; Hockless, D. C. R.; Glen, A. D.; Richards, D. G. *J. Chem. Soc., Chem. Commun.* **1990**, 1565.
(32) Du, M.; Guo, Y.-M.; Chen, S.-T.; Bu, X.-H. *Inorg. Chem.* **2004**, *43*, 1287.
(33) Xia, J.; Shi, W.; Chen, X.-Y.; Wang, H.-S.; Cheng, P.; Liao, D.-Z.; Yan, S.-P. *Dalton Trans.* **2007**, 2373–2375.
(34) Zhang, W.-H.; Song, Y.-L.; Zhang, Y.; Lang, J.-P. *Cryst. Growth Des.* **2008**, *8*, 253.
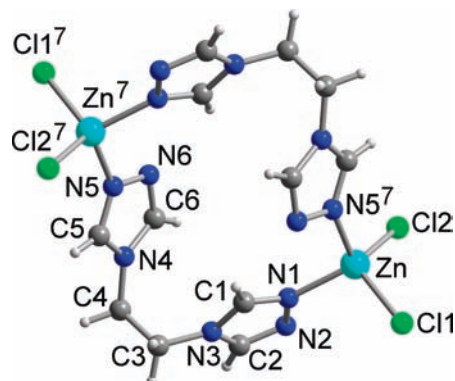
Figure 1. Dinuclear molecular structure in **1** and **2** (Br instead of Cl in **2**). Selected distances and angles in Table S4, Supporting Information, ranges in Table 1. Symmetry code in **1** and **2**: 7 = 0.5 − x, 1.5 − y, 1 − z.
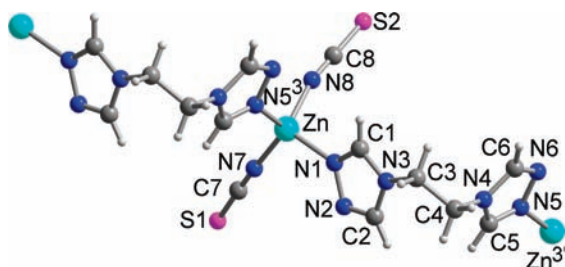
Figure 2. Coordination environment of the zinc atom in **3**. Selected distances and angles in Table S5, Supporting Information, ranges in Table 1. Symmetry codes: 3 = 0.5 + x, 0.5 + y, z; 3′ = −0.5 + x, −0.5 + y, z.

organized by C−H···N[35,36] and C−H···X (X = Cl,[35,37] Br[38]) hydrogen bonds (Table S1, Supporting Information).

$^1_\infty$**[Zn(NCS)$_2$(μ_2-btre)] 3.** The tetrahedral zinc atom in **3** is coordinated by two nitrogen atoms from two cis-bent bridging btre ligands and two nitrogen atoms from two terminal isothiocyanato groups (Figure 2). As in **1** and **2** only one nitrogen atom on each triazole ring is used for metal coordination in a μ_2-btre-$\kappa N1{:}N1'$ mode. Each btre ligand bridges between two zinc atoms. The resulting corrugated strands are interconnected through C−H···N hydrogen bonds (Figure 3, Table S1, Supporting Information).[35,36]

$^2_\infty$**[Cu$_2$(μ_2-Cl)$_2$(μ_4-btre)] 4 and $^2_\infty$[Cu$_2$(μ_2-Br)$_2$(μ_4-btre)] 5.** The isomorphous copper(I) compounds **4** and **5** feature a dinuclear metal unit in which inversion symmetry related

(35) (a) Desiraju, G. R.; Steiner, T. The weak hydrogen bond. In *IUCr Monograph on Crystallography*; Oxford Science: Oxford, 1999; Vol. 9. (b) Desiraju, G. R. *Acc. Chem. Res.* **2002**, *35*, 565. (c) Mascal, M. *Chem. Commun.* **1998**, 303.
(36) Janiak, C.; Scharmann, T. G. *Polyhedron* **2003**, *22*, 1123.
(37) (a) Wisser, B.; Janiak, C. *Z. Anorg. Allg. Chem.* **2007**, *633*, 1796–1800. (b) Fun, H. K.; Chantrapromma, S.; Lu, Z. L.; Neverov, A. A.; Brown, R. S. *Acta Crystallogr.* **2006**, *E62*, m3225−m3227. (c) Gunay, M. E.; Aygun, M.; Kartal, A.; Cetinkaya, B.; Kendi, E. *Cryst. Res. Technol.* **2006**, *41*, 615–621. (d) Wang, X. F.; Deng, S. L.; Long, L. S.; Huang, R. B.; Zheng, L. S. *J. Incl. Phenom. Macrocycl. Chem.* **2006**, *54*, 295–298. (e) Ban, S. R.; Yang, X.; Chen, W. B.; Cheng, X. F.; Song, H. B. *Acta Crystallogr.* **2006**, *E62*, o1713−o1714. (f) Lorono-Gonzalez, D. *Acta Crystallogr.* **2006**, *E62*, o1735−o1737. (g) Balamurugan, V.; Mukheriee, R. *Inorg. Chim. Acta* **2006**, *359*, 1376–1382. (h) Xu, H.; Song, Y.-L.; Mi, L.-W.; Hou, H-W.; Tang, M.-S.; Sang, Y.-L.; Fan, Y.-T.; Pan, Y. *Dalton Trans.* **2006**, 838–845. (i) Ravikumar, K.; Sridhar, B.; Mahesh, M.; Reddy, V. V. N. *Acta Crystallogr.* **2006**, *E62*, o318−o320.
(38) (a) Zhang, W.; Tang, X.; Ma, H.; Sun, W.-H.; Janiak, C. *Eur. J. Inorg. Chem.* **2008**, 2830–2836. (b) Neve, F.; Crispini, A. *Cryst. Growth Des.* **2001**, *1*, 287–393.

Table 1. Ranges of Bonds Lengths (Å) and Angles (deg) in **1−10**

	1 (X = Cl)	**2** (X = Br)
Zn−N	2.007−2.015	2.005−2.012
Zn−X	2.214−2.241	2.352−2.371
N−Zn−N	103.76(5)	104.26(11)
N−Zn−X	108.14−113.48	107.77−113.04
X−Zn−X	113.38(2)	112.36(2)

	3	
Zn−N	1.922−2.005	
N−C (NCS)	1.164−1.166	
C−S	1.614−1.615	
N−Zn−N	101.0−113.7	
Zn−N−C(S)	167.7−170.6	

	4 (X = Cl)	**5** (X = Br)
Cu−N	2.007−2.038	2.009−2.024
Cu−X	2.343−2.439	2.4616−2.5620
Cu···Cu	3.027−3.616(1)	3.176−3.611(4)
N−Cu−N	112.4(1)	112.25(7)
N−Cu−X	105.6−120.9	103.61−114.62
X−Cu−X	101.48(4)	101.59(1)
Cu−X−Cu	78.52(4)	78.41(1)

	6	
Cd−O	2.257−2.354	
Cd−N	2.299−2.347	
N−Cd−N	169.1−177.0	
N−Cd−O	85.1−97.8	
O−Cd−O	cis: 75.7−122.8	

	7	
Cu−N	1.996−2.075	
N−Cu−N	94.95−117.52	

	8 (M = Zn)	**9** (M = Cd)
M−N	2.159−2.210	2.327−2.353
cis N−M−N	86.4−93.2	87.9−91.8
trans N−M−N	179.0−179.8	178.2−178.7

|	**10**	
Cu−C	1.906(3)	
Cu−N	1.998−2.084	
C−N (cyanide)	1.145(4)	
N−Cu−N	101.0−106.4	
N−Cu−C	110.3−119.6	
Cu−C−N(CN)	173.6(3)	
Cu−N−C(CN)	165.7(2)	

Cu atoms are bridged by two halogen anions or two triazolyl rings. Thus, two halogen and two nitrogen atoms coordinate the copper(I) atom in a tetrahedral fashion. Each trans-bent btre ligand connects four copper atoms in $\kappa N1{:}N2{:}N1'{:}N2'$ mode and each halide ligand bridges between two Cu atoms to give 2D nets (Figure 4 and 5).

Neighboring layers are connected through C−H···X (X = Cl,[35,37] Br[35,38]) hydrogen bonds (Figure 6, Table S2, Supporting Information,) and strong π-π interactions[39] between the triazolyl rings (Figure 6, Table S3, Supporting Information).

$^2_\infty$**{[Cd$_6$(μ_3-OH)$_2$(μ_3-SO$_4$)$_4$(μ_4-btre)$_3$(H$_2$O)$_6$](SO$_4$)·∼6H$_2$O} 6.** The cadmium compound **6** features a trinuclear and triangular metal unit with three crystallographically different cadmium sites (Figure 7). Each Cd atom has an octahedral environment of four oxygen atoms and two trans nitrogen atoms.[40] The three Cd atoms are bridged by a μ_3-hydroxo and a μ_3-sulfato group below and above the Cd$_3$-plane (cf. Scheme 2).[41] Along the edges of the Cd$_3$ triangle three crystallographically different
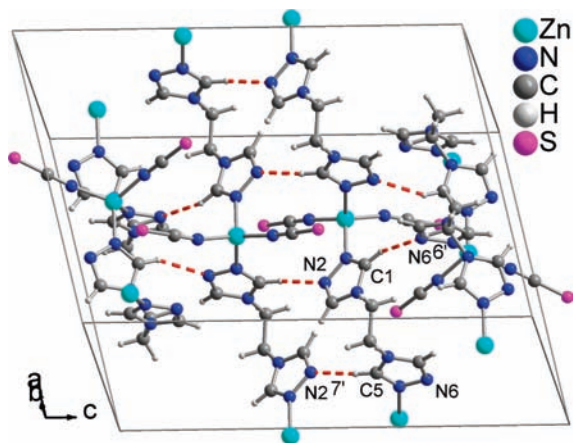
Figure 3. Packing diagram for **3** showing four [Zn(NCS)₂(μ₂-btre)] strands with C—H⋯N bonding as dashed lines. The C5—H⋯N2 bonding connects two adjacent strands (the two middle ones) along their full length (see Table S1, Supporting Information, for details).
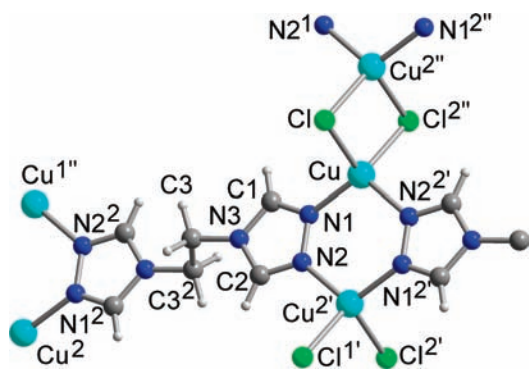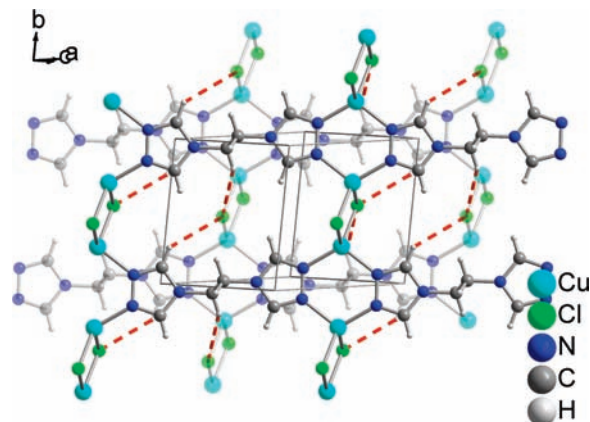

Figure 4. Coordination environment of the copper atom in **4** and **5** (Br instead of Cl in **5**). Selected distances and angles in Table S6, Supporting Information, ranges in Table 1. Symmetry codes in **4** and **5**: 1 = *x*, −1 + *y*, *z*; 1′ = *x*, −1 + *y*, *z*; 1″ = −1 + *x*, *y*, −1 + *z*; 2 = −*x*, −*y*, 1 − *z*; 2′ = 1 − *x*, −*y*, 1 − *z*; 2″ = 1 − *x*, 1 − *y*, 2 − *z*.
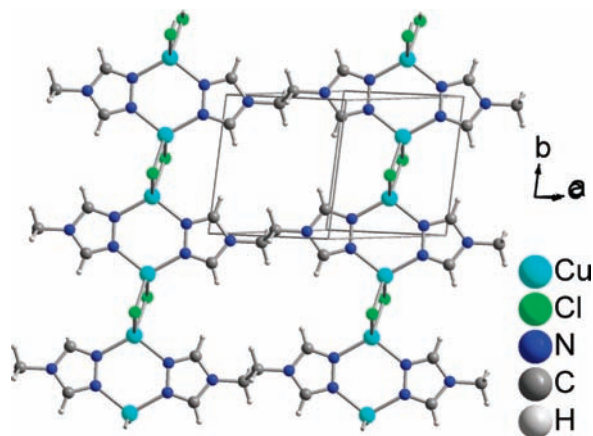
Figure 5. 2D network in **4** and **5** (Br instead of Cl in **5**).

triazolyl rings bridge between adjacent Cd atoms in κ*N*1:*N*2 mode. The coordination sphere of Cd1 is concluded by two oxygen atoms from two other symmetry-related μ₃-sulfato groups which connect three different Cd₃ units (cf. Figure 8a). The environment of Cd2 is concluded by an oxygen atom of one of these μ₃-sulfato groups and an aqua ligand. The coordination sphere Cd3 is concluded by two aqua ligands

(39) Janiak, C. *J. Chem. Soc., Dalton Trans.* **2000**, 3885.

Figure 6. Packing diagram of **4** and **5** (Br instead of Cl in **5**) showing two neighboring layers (the one in the rear is depicted semi-transparent) connected through C—H⋯X (X = Cl, Br) hydrogen bonds as dashed lines and π-π interactions between triazolyl rings. Note the almost perfect face-to-face stacking of the symmetry related parallel triazolyl rings in the middle of the picture (for details see Tables S2 and S3, Supporting Information).
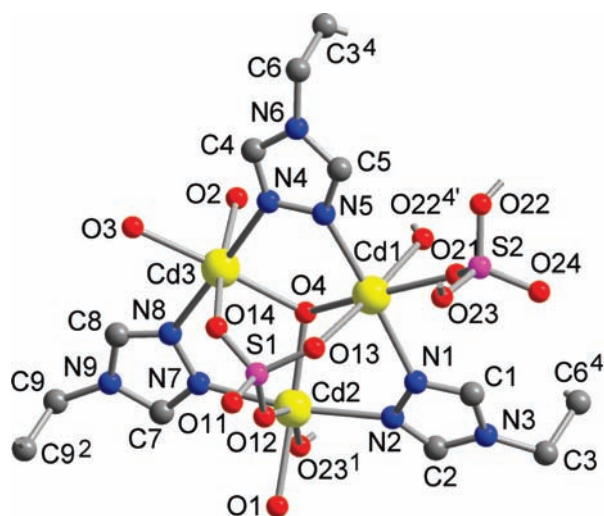
Figure 7. Trinuclear cadmium unit in **6**; hydrogen atoms not shown for clarity. Selected distances and angles in Table S7, Supporting Information, ranges in Table 1. Symmetry codes: 1 = *x*, −1 + *y*, *z*; 2 = 1 − *x*, *y*, 0.5 − *z*; 4 = 0.5 − *x*, 0.5 + *y*, 0.5 − *z*; 4′ = 0.5 − *x*, −0.5 + *y*, 0.5 − *z*.

(Figure 7). The structure contains two symmetrically different btre ligands, one of them with symmetry related triazolyl halves. Each btre ligand is cis-bent and connects four cadmium atoms in κ*N*1:*N*2:*N*1′:*N*2′ mode (cf. Figure 8b).
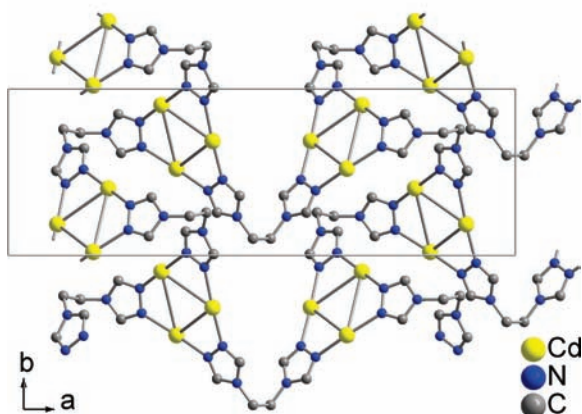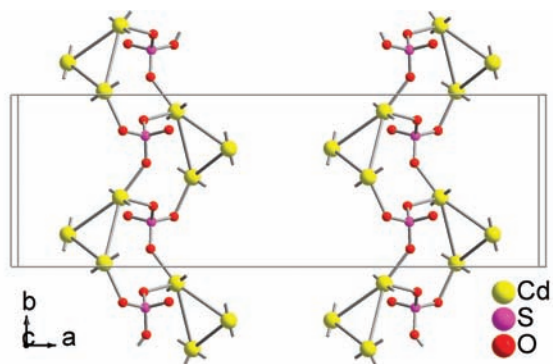
The trinuclear and triangular Cd₃ units are bridged by μ₃-sulfato groups into 1D strands (Figure 8a). The 2D network in **6** arises solely through the bridging action of the btre ligands between the Cd₃ units (Figure 8b). In between adjacent layers lie water molecules of crystallization and, for charge balance, a half-occupied and disordered, non-coordinated sulfate anion (near an inversion center, Figure 9).

³∞{[Cu(μ₄-btre)]ClO₄·~0.25H₂O} **7**. The copper(I) atom in **7** is tetrahedrally coordinated by four nitrogen atoms from

(40) (a) Banerjee, S.; Ghosh, A.; Wu, B.; Lassahn, P.-G.; Janiak, C. *Polyhedron* **2005**, *24*, 593–599. (b) Banerjee, S.; Lassahn, P.-G.; Janiak, C.; Ghosh, A. *Polyhedron* **2005**, *24*, 2963–2971.
(41) Deng, H.; Qiu, Y.-C.; Li, Y.-H.; Liu, Z.-H.; Zeng, R.-H.; Zeller, M.; Batten, S. R. *Chem. Commun.* **2008**, 2239–2241.

Figure 8. Packing analysis for **6** by differentiation in individual (a) {Cd-SO$_4$}-strands and (b) {Cd-btre}-nets; hydrogen atoms not shown. The connecting lines between the Cd atoms in a Cd$_3$ unit are topological aids.
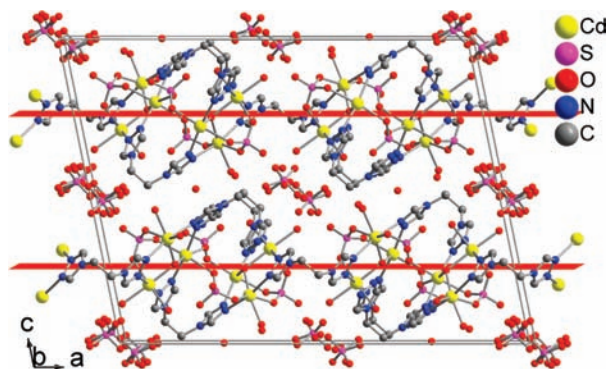

Figure 9. Packing diagram for **6** viewed along 2D layers, parallel to the (0 0 4) planes (indicated in red) to show the disordered, non-coordinated sulfate anions between the layers.

four bridging btre ligands (Figure 10). Neighboring, inversion-symmetry related Cu atoms are bridged by two triazolyl rings to give metal strands along *c* (Figure 11). The trans-bent btre ligand with *C$_2$*-symmetry related triazolyl moieties connects four copper atoms in $\kappa N1{:}N2{:}N1'{:}N2'$ mode to create an open 3D framework with rhombic channels (Figure 11) which contains the rotationally disordered perchlorate ions and some crystal water.

$^3_\infty${[Zn(μ_4-btre)(μ_2-btre)](ClO$_4$)$_2$} **8** and $^3_\infty${[Cd(μ_4-btre)(μ_2-btre)](ClO$_4$)$_2$} **9.** In the isomorphous compounds **8** and **9** the zinc or cadmium metal atom, respectively, is octahedrally coordinated by six nitrogen atoms from six bridging btre ligands (Figure 12). Symmetry related neighboring metal atoms are
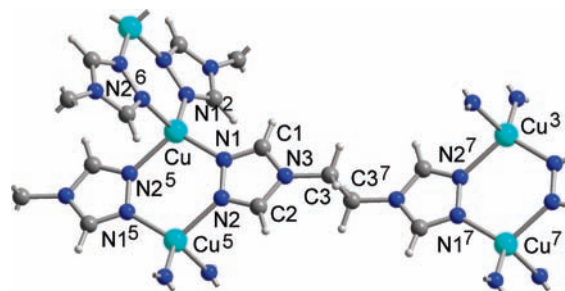
Figure 10. Coordination environment of the copper atom in **7**. Selected distances and angles in Table S8, Supporting Information, ranges in Table 1. Symmetry codes: 3 = 0.5 + *x*, 0.5 + *y*, *z*; 2 = −*x*, *y*, 0.5 − *z*; 5 = −*x*, −*y*, −*z*; 6 = *x*, −*y*, 0.5 + *z*; 7 = 0.5 − *x*, 0.5 − *y*, −*z*.
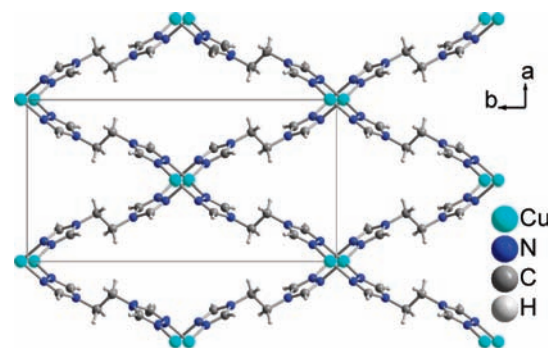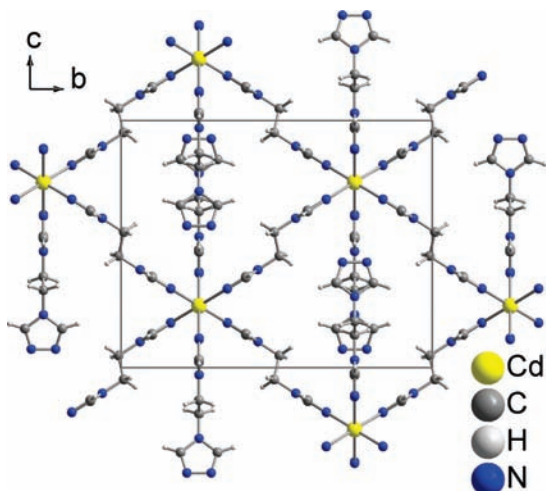

Figure 11. 3D framework in **7**. Disordered perchlorate ions and crystal water in channels are not shown for clarity (filled network in Figure S24, Supporting Information).
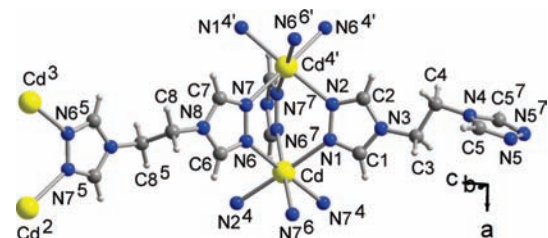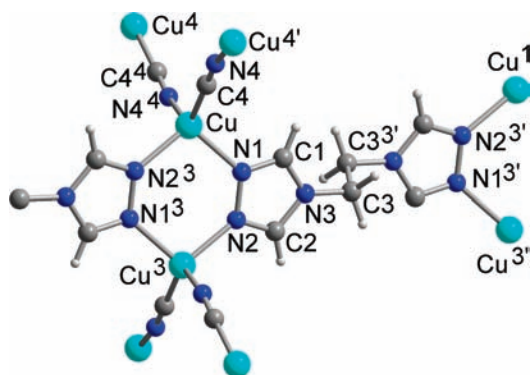

Figure 12. Coordination environment of the metal atom in **8** and **9** (Zn instead of Cd in **8**). Selected distances and angles in Table S9, Supporting Information, ranges in Table 1. Symmetry codes: 2 = 0.5 − *x*, 1 − *y*, 0.5 + *z*; 3 = −*x*, 0.5 + *y*, 1 − *z*; 4 = 0.5 + *x*, 0.5 − *y*, 0.5 − *z*; 4′ = −0.5 + *x*, 0.5 − *y*, 0.5 − *z*; 5 = −*x*, 1 − *y*, 1 − *z*; 6 = 0.5 + *x*, *y*, 0.5 − *z*; 6′ = −0.5 + *x*, *y*, 0.5 − *z*; 7 = *x*, 0.5 − *y*, *z*.

bridged by three triazolyl rings to give metal strands along *a* (Figure 12). There are two crystallographically different btre ligands in these structures. The trans-bent ligand with triazol ring N6−N8 and inversion-symmetry related triazolyl moieties connects four metal atoms in the typical $\kappa N1{:}N2{:}N1'{:}N2'$ mode, as seen before, and gives rise to a 3D framework (Figure 13). The trans-bent ligand with rings N1−N3 and N4−N5 connects only between two metal atoms in the novel $\kappa N1{:}N2$ mode and has a non-coordinating triazole ring (N4−N5). Ring N1−N3 lies on a special position within a symmetry plane, and the triazole ring N4−N5 is bisected by this plane of symmetry. Both triazol rings of this special btre ligand are, thus, rotated 90° to each other. This dangling btre ligand reaches into the rhombic channels of the 3D framework (Figure 13). Dangling btre ligands from opposite corners interdigitate with C−H···N bonding (Table S1, Supporting Information), thereby separating the rhombic channels into two trigonal halves which contain

Figure 13. 3D framework in in **8** and **9** (Zn instead of Cd in **8**). Perchlorate ions in the trigonal channels are ordered but are not shown for clarity (filled network in Figure S25, Supporting Information).


Figure 14. Coordination environment of the copper atom in **10**. Selected distances and angles in Table S10, Supporting Information, ranges in Table 1. Symmetry codes: $1 = 1 + x, y, -1 + z$; $3 = -x, 1 - y, 1 - z$; $3' = 1 - x, 1 - y, -z$; $4 = -0.5 + x, 1.5 - y, -0.5 + z$; $4' = 0.5 + x, 1.5 - y, 0.5 + z$.

the ordered perchlorate ions (C−H···O bonding, Table S1, Supporting Information).

$_{\infty}^{3}[\text{Cu}_2(\mu_2\text{-CN})_2(\mu_4\text{-btre})]$ **10.** The copper(I) atom in **10** is coordinated by two nitrogen atoms from two btre ligands, one cyano nitrogen, and one cyano carbon atom (Figure 14). The cyano groups are a decomposition product from the btre ligand in the hydrothermal synthesis, concomitant with the reduction from Cu(II) to Cu(I). Each cyano ligand bridges between two Cu atoms. Adjacent copper(I) atoms are either connected by a close to linear cyanide bridge or by two triazolyl rings to a six-membered Cu_2N_4 ring with inversion symmetry. These bridging actions create a 2D subnet with larger openings (Figure 15). Furthermore, each trans-bent btre ligand has inversion-symmetry related triazolyl moieties and connects four copper atoms (cf. Figure 14) from adjacent 2D subnets in $\kappa N1{:}N2{:}N1'{:}N2'$ mode to give an open 3D framework (Figure 16).

The wide openings in the single 3D framework shown in Figure 16 lead to the 2-fold intepenetration of two symmetry-related 3D networks to give a densely packed structure.[1] The interpenetration or internetwork packing is controlled by a
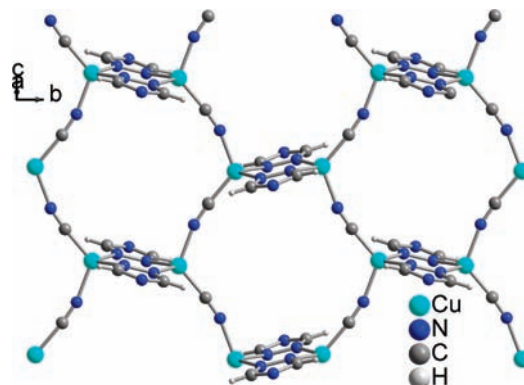
Figure 15. 2D subnet in **10** from the bridging action of the cyano groups and the triazolyl rings between the copper atoms; the remainder to each triazolyl ring is not shown for clarity.
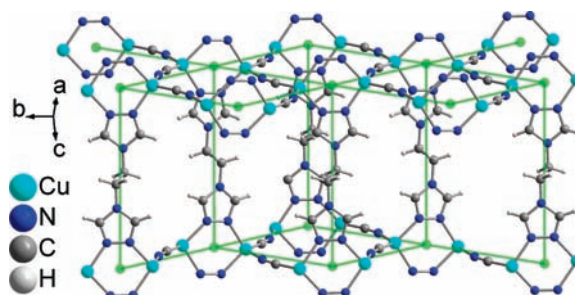
Figure 16. One of the interpenetrating 3D frameworks in **10** (cf. Figure 17). Centroids of the six-membered Cu_2N_4 rings are shown as green balls and with connecting lines (semitransparent) to better visualize the open 3D framework.
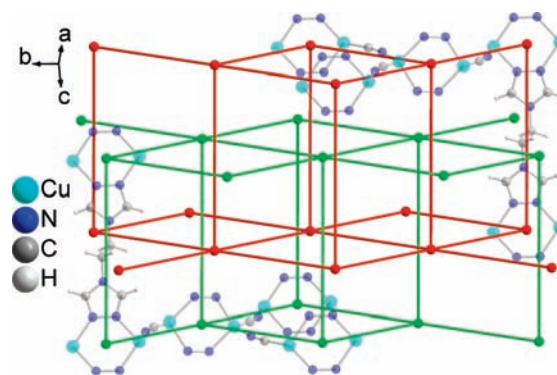
Figure 17. Schematic drawing of the two interpenetrating 3D frameworks in **10** (one in green and the other in red). Centroids of the six-membered Cu_2N_4 rings are given as green or red balls and with connecting lines.

typical π-stacking interaction (Figure 18, Table S3, Supporting Information).[39,42]

Solid-State CPMAS NMR. The number of crystallographically (symmetry) independent (unique) atoms of the asymmetric unit in (diamagnetic) compounds and coordination networks should be reflected in the solid-state NMR spectra of active nuclei.[43,44] A collection of solid-state NMR

(42) Wu, H.-P.; Janiak, C.; Uehlin, L.; Klüfers, P.; Mayer, P. *Chem. Commun.* **1998**, 2637–2638.
(43) Chierotti, M. R.; Gobetto, R. *Chem. Commun.* **2008**, 1621–1634.
(44) (a) Ruiz, J.; Rodríguez, V.; Cutillas, N.; Hoffmann, A.; Chamayou, A.-C.; Kazmierczak, K.; Janiak, C. *CrystEngComm* **2008**, *10*, 1928–1938. (b) Habib, H. A.; Hoffmann, A.; Höppe, H. A.; Janiak, C. *Dalton Trans* **2009**, DOI: 10.1039/b812670d. (c) Althoff, G.; Ruiz, J.; Rodríguez, V.; López, G.; Pérez, J.; Janiak, C. *CrystEngComm* **2006**, *8*, 662–665.
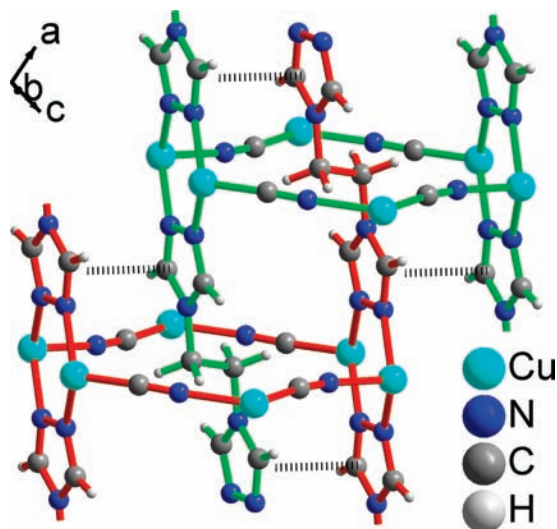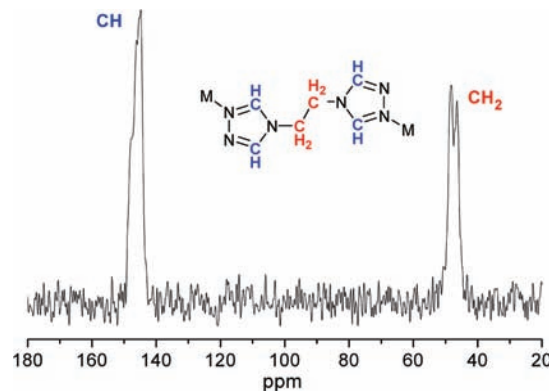
Figure 18. Interpenetration of the two 3D frameworks (differentiated by the green and red bonds) through the grid windows in **10** with indication of the controlling π-π stacking interaction (dashed lines) of the (by symmetry relation $1 - x$, $1 - y$, $1 - z$) parallel triazolyl rings: Centroid−centroid distance 3.505(2) Å, interplanar separation 3.25 Å, slippage 1.32 Å (= parallel displacement between ring centroids from a perfect face-to-face alignment, cf. Table S3, Supporting Information).

Figure 19. ^{13}C CPMAS NMR spectrum for **2** (as an example also for **1**) and schematic drawing of the building unit with the unique C atoms given as atom symbols. The four symmetry different triazolyl-CH carbon atoms are not resolved. Peak positions: 144.8, 48.2, and 46.4 ppm.

Figure 20. ^{13}C CPMAS NMR spectrum for **3** and schematic drawing of the building unit with the unique C atoms as atom symbols. Peak positions: 150.7, 149.8, 146.4, 142.3, 138.3, 48.3, and 44.2 ppm.
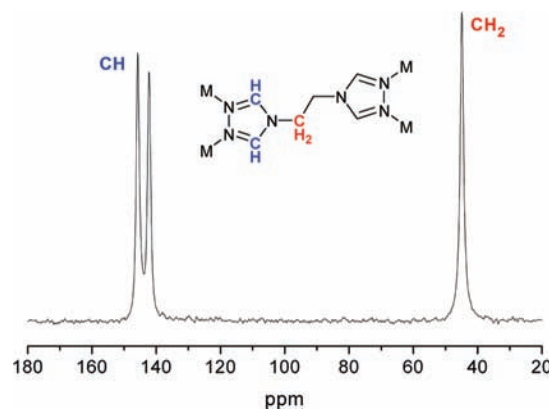
Figure 21. ^{13}C CPMAS NMR spectrum for **7** (example also for **4** and **5**) and schematic drawing of the building unit with the unique C atoms as atom symbols. Peak positions: 145.8, 142.2, and 44.9 ppm.

spectra for a certain ligand or ligand combination could eventually serve as a tool to elucidate, without single-crystal X-ray crystallography, the network topology, the nature and stereochemistry of hitherto structurally uncharacterized solids, amorphous or poorly crystalline coordination polymers.[45] Also, solid-state NMR can be a structurally informative technique for materials containing stoichiometric paramagnetic Cu(I)/Cu(II)/Zn(II) constituents.[46] Structural studies in the solid state by ^{13}C and ^{15}N CPMAS NMR spectroscopy carried out on a series of 2-aminotroponimine derivatives have allowed to establish the existence of hydrogen bonding and to determine the most stable tautomer.[47] So far, we are not aware of many in-depth solid-state NMR investigations of metal-organic coordination networks.
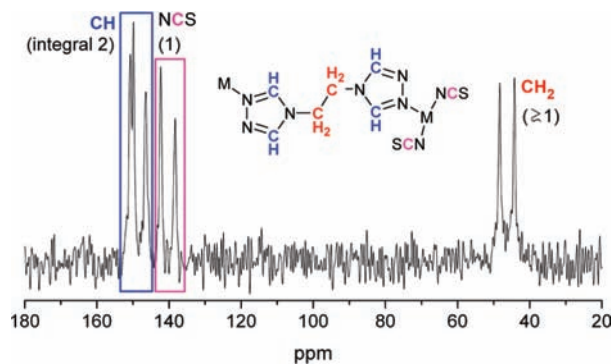
Generally, the ^{13}C CPMAS spectra of the diamagnetic metal-btre complexes **1−10** exhibit CH resonances between 142−149 ppm (btre ligand 145.6 ppm, cf. Figure S26, Supporting Information) and CH$_2$ resonances usually between 44−49 ppm (btre ligand 44.1 ppm). The dihalozinc compounds **1** and **2** (0D) with a μ_2-btre-$\kappa N1$:$N1'$ coordination mode (cf. Figure 1, Figure 19) give ^{13}C CPMAS spectra with a notably lower signal-to-noise ratio. Such an increased noise could also be seen in the halocopper nets **4** and **5** and is ascribed to the presence of the halogen quadrupolar nuclei (vide infra).

The ^{13}C CPMAS NMR spectrum of the 1D di(isothiocyanato)zinc chain **3** with μ_2-btre-$\kappa N1$:$N1'$ mode has almost the expected number of different C atoms resolved, with the zinc-bound NCS signals in the expected region (Figure 20).[48]

Compound **4**, **5**, and **7** with a μ_4-btre coordination mode and half a ligand unique, that is, one symmetry-independent triazolyl-methylene group (cf. Figure 4 and 10), display the three signals expected for the three symmetry-different carbon atom (Figure 21).

The ^{13}C CPMAS spectrum of **6** (Figure 22) displays 5 out of 9 signals expected for the symmetry-independent carbon atoms of a full and half a unique btre ligand, with both of them in μ_4-bridging mode (cf. Figure 7).

Compound **8** and **9** contain in 1:1 ratio a μ_4- (half-unique) as well as a μ_2-$\kappa N1$:$N2$-bridging (dangling) btre ligand

(45) Masciocchi, N.; Galli, S.; Alberti, E.; Sironi, A.; Di Nicola, C.; Pettinari, C.; Pandolfo, L. *Inorg. Chem.* **2006**, *45*, 9064–9074.

(46) Ouyang, L.; Aguiar, P. M.; Batchelor, R. J.; Kroeker, S.; Leznoff, D. B. *Chem. Commun.* **2006**, 744–746.

(47) Claramunt, R. M.; Sanz, D.; Pérez-Torralba, M.; Pinilla, E.; Torres, M. R.; Elguero, J. *Eur. J. Org. Chem.* **2004**, 4452–4466.

Figure 22. ^{13}C CPMAS NMR spectrum for **6** and schematic drawing of the building unit with the unique C atoms as atom symbols. Peak positions: 146.7, 145.4, 143.3, 142.2, and 47.7 ppm.

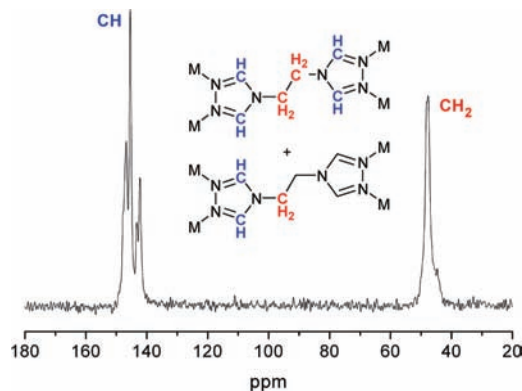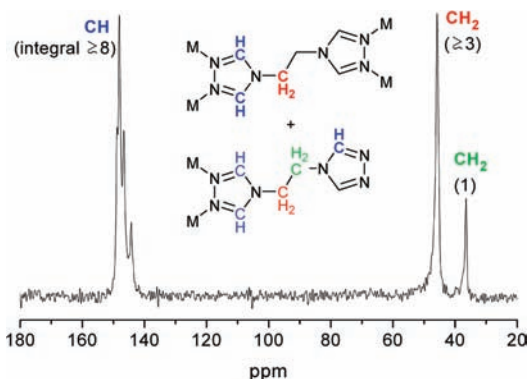**Figure 23.** ^{13}C CPMAS NMR spectrum for **8** (example also for **9**) and schematic drawing of the building unit with the unique C atoms as atom symbols. All atoms of the μ_2-$\kappa N1$:$N2$-bridging, dangling btre ligand have half-occupancy (indicated by plain font style). Integral of CH_2 resonance around 37 ppm set to 1. Peak positions: 148.8, 148.1, 146.6, 144.2, 45.7, and 36.5 ppm (148.4, 147.6, 146.3, 144.3, 45.6, and 37.2 ppm for **9**, cf. Figure S27, Supporting Information).
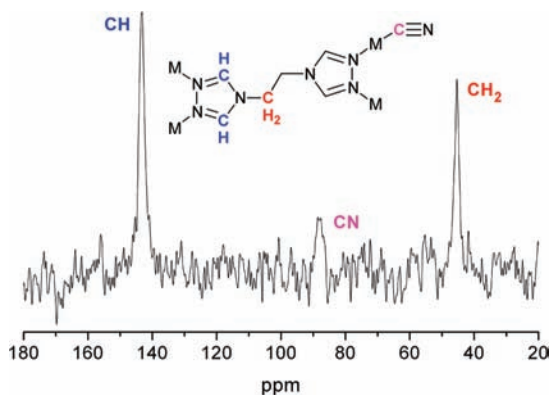
Figure 24. ^{13}C CPMAS NMR spectrum for **10** and schematic drawing of the building unit with the unique C atoms as atom symbols. Peak positions: 143.3 (broad but not spiked), 88.6, and 45.4 ppm.

(within and bisected by a mirror plane, cf. Figure 12) and show 6 out of 8 signals expected for the symmetry-different (unique) carbon atoms (Figure 23). The special case of the μ_2-$\kappa N1$:$N2$-btre ligand gives rise to a new signal at high field, around 37 ppm, which is not seen in any other ^{13}C CPMAS NMR spectra of the metal-btre complexes or the free btre ligand (cf. Figure S26). Repeated NMR experiments on different batches (Figure S27, Supporting Information) ruled out that it originates from any impurities. Furthermore, the
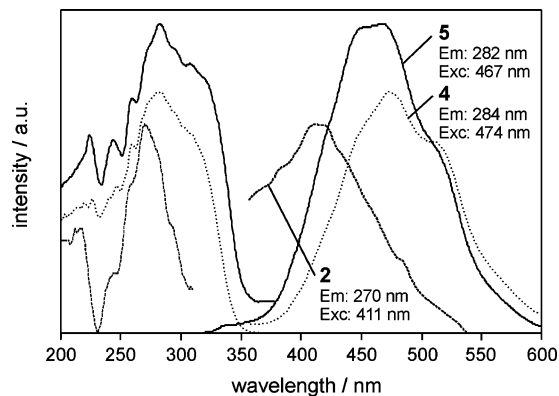
Figure 25. Fluorescence excitation and emission spectra of **2**, **4**, and **5**; the respective excitation (emission spectra) and monitored wavelengths (excitation spectra) are indicated.

integral ratio of this upfield-shifted CH_2 resonance to the other signal groups matches the expected ratio of 8 (CH) to 3 (remaining three CH_2) to 1 (CH_2). Noteworthy, a chemical shift difference of 8−9 ppm between the CH_2 resonances is unusually large for otherwise chemically very similar groups. We assign this CH_2 resonance below 40 ppm to the CH_2 group bound to the uncoordinated triazolyl ring (C4, cf. Figure 12) as the bonding angle (C3−C4−N4) at this carbon atom is only 106.9(4)°. Its neighboring methylene group (C3) has a bonding angle of 113.8(4)°. The other btre-methylene groups in **1**−**10** and in the benzene-1,3,5-tricarboxylate adduct of btre[15] lie between 109.6(4)° and 113.8(3)°, typically being somewhat widened relative to the tetrahedral angle. Angular distortions can affect the MAS chemical shift.[49] Also, the CH_2 group bound to the uncoordinated triazolyl ring may come close to the shielding region of a nearby triazolyl group from an interdigitated dangling btre ligand (cf. Figure 13).

The cyanide framework **10** features again a μ_4-coordination mode with half a btre ligand being unique. Its ^{13}C CPMAS spectrum (Figure 24) shows 2 out of 3 signals expected for the three symmetry-independent triazolyl-methylene carbon atoms, plus the signal for the cyano carbon atom.

The ^{1}H MAS NMR spectra feature broader peaks and hence are less susceptible to a direct interpretation. Yet, they follow in resolution and differing patterns the ^{13}C spectra (cf. Figures S28−S38, Supporting Information).

It is obvious that different metal-btre coordination modes give rise to different signal patterns in the ^{13}C CPMAS NMR spectra from which, in turn, the metal−ligand substructure can be deduced. The ligand symmetry is clearly visible through the number of peaks. Furthermore increased splittings (cf. Figure 20) or enhanced chemical shifts (cf. Figure 23) in comparison to similar spectra are evidence for packing effects. The latter cannot yet be traced to a simple origin. To understand and quantify the different effects possible in the solid state a more thorough analysis of the chemical shifts

(48) Fratiello, A.; Kubo-Anderson, V.; Lee, D. J.; Mao, T.; Ng, K.; Nickolaisen, S.; Perrigan, R. D.; San Lucas, V.; Tikkanen, W.; Wong, A.; Wong, K. *J. Solution Chem.* **1998**, *27*, 331–359.

(49) Sebastini, D. *Int. J. Quantum Chem.* **2005**, *101*, 849–853. Alam, T. M.; Friedmann, T. A.; Schultz, P. A.; Sebastiani, D. *Phys. Rev.B* **2003**, *67*, 245309.
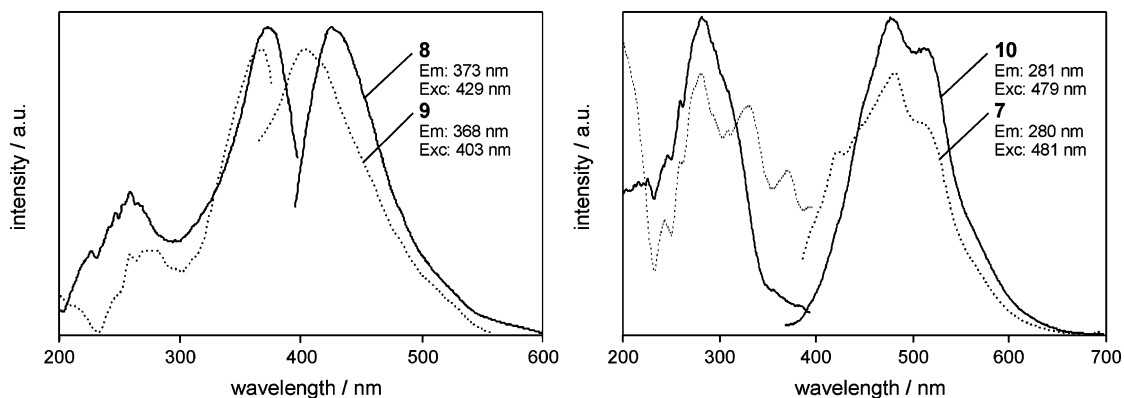
Figure 26. Fluorescence excitation and emission spectra of **7**, **8**, **9**, and **10**; the respective excitation (emission spectra) and monitored wavelengths (excitation spectra) are indicated.

Table 2. Crystal Data and Structure Refinement for **1**−**3**

compound	1	2	3
empirical formula	$C_{12}H_{16}Cl_4Zn_2N_{12}$	$C_{12}H_{16}Br_4Zn_2N_{12}$	$C_8H_8ZnN_8S_2$
M/g mol^{-1}	600.91	778.75	345.71
crystal size/mm	0.41 × 0.29 × 0.04	0.32 × 0.18 × 0.03	0.23 × 0.12 × 0.05
2θ range/deg	6.42−72.64	4.12−58.02	4.34 − 51.70
h; k; l range	−32, 29; −11, 10; −24, 27	±26; ± 9; −22, 23	±18; −11, 10; ± 23
crystal system	monoclinic	monoclinic	monoclinic
space group	$C2/c$	$C2/c$	$C2/c$
a/Å	19.7337(4)	19.9430(6)	14.898(2)
b/Å	6.71120(10)	6.9223(2)	9.514(1)
c/Å	16.7151(3)	16.9212(5)	19.584(2)
α/deg	90.00	90.00	90.00
β/deg	97.4060(10)	97.101(3)	106.316(2)
γ/deg	90.00	90.00	90.00
V/Å^3	2195.23(7)	2318.08(12)	2664.2(6)
Z	4	4	8
D_{calc}/g cm^{-3}	1.818	2.231	1.724
F (000)	1200	1488	1392
μ/mm^{-1}	2.700	8.991	2.155
max/min transmission	0.8997/0.4041	0.7742/0.1610	0.8999/0.6370
reflections collected (R_{int})	14437 (0.0255)	23706 (0.0753)	11194 (0.0634)
independent reflections	4979	3081	2441
obs. reflect. [$I > 2\sigma(I)$]	3877	2180	1824
parameters refined	136	136	172
max./min. $\Delta\rho^a$/e Å^{-3}	0.476/−0.576	0.647/−0.751	0.427/−0.379
R_1/wR_2 [$I > 2\sigma(I)$]^b	0.0303/0.0676	0.0335/0.0573	0.0367/0.0690
R_1/wR_2 (all reflect.)^b	0.0460/0.0727	0.0634/0.0652	0.0577/0.0774
Goodness-of-fit on F^{2c}	1.020	0.999	1.040
weight. scheme w; a/b^d	0.0351/0.4069	0.0242/1.7857	0.0268/2.6630

^{a} Largest difference peak and hole. ^{b} $R_1 = [\sum(||F_o| - |F_c||)/\sum|F_o|]$; $wR_2 = [\sum[w(F_o^2 - F_c^2)^2]/\sum[w(F_o^2)^2]]^{1/2}$. ^{c} Goodness-of-fit = $[\sum [w(F_o^2 - F_c^2)^2]/(n - p)]^{1/2}$. ^{d} $w = 1/[\sigma^2(F_o^2) + (aP)^2 + bP]$ where $P = (\max(F_o^2 \text{ or } 0) + 2F_c^2)/3$.

by quantum chemical calculations or the systematic investigation of many more systems is needed.

Luminescence Properties. The compounds **2**, **4**, **5**, **7**, **8**, **9**, and **10** exhibit broadband luminescence under UV excitation (Figures 25 and 26). The free ligand btre did not show fluorescence probably because of a photoinduced electron transfer.[50]

The dinuclear molecular zinc complex exhibits only luminescence if coordinated to bromide (compound **2**). Under excitation at 270 nm an emission at 411 nm was observed. The chloride compound **1** did not show any measurable luminescence. Both copper(I) halide centered 2D coordination polymers **4** and **5** show strong blue luminescence peaking around 470 nm upon excitation at 282 and 284 nm.

The relative intensity of the chloride containing **4** is weaker compared with that of the bromide one (**5**). No luminescence was found for the cadmium sulfate network **6** probably mainly because of quenching as a consequence of high-frequency oscillations of OH-groups directly coordinated to cadmium. This observation is made frequently in the case of rare earth ions when multiples of the oscillation strength of the OH group approximately match the energy of the radiative emission.[51,52] Additionally, one rather often observes a significant decrease of fluorescence intensity caused by the coordination of complex ions to heavier atoms like cadmium(II) because of the heavy-atom effect. With increasing atom number these ions promote intersystem crossings leading to quenching of fluorescence and in some cases increasing phosphorescence.[53] This fits very nicely with our results which show more intense fluorescence of the copper(I)

(50) Ji, H. F.; Dabestani, R.; Brown, G. M.; Hettich, R. L. *Photochem. Photobiol.* **1999**, *69*, 513.

Table 3. Crystal Data and Structure Refinement for **4**−**7**

compound	4	5	6	7
empirical formula	$C_3H_4ClCuN_3$[e]	$C_3H_4BrCuN_3$[e]	$C_9H_{25}Cd_3N_9O_{17}S_{2.5}$[e,f]	$C_6H_{8.5}ClCuN_6O_{4.25}$[g]
M/g mol^{-1}	181.08	225.54	948.73[f]	331.67[e]
crystal size/mm	$0.38 \times 0.24 \times 0.04$	$0.22 \times 0.07 \times 0.02$	$0.44 \times 0.24 \times 0.05$	$0.45 \times 0.28 \times 0.03$
2θ range/deg	6.26−53.88	5.90−56.78	3.96−53.8	4.74 − 52.96
h; k; l range	$\pm8; \pm 8; \pm 8$	$\pm8; \pm 8; \pm 9$	$\pm35; \pm 11; \pm 27$	$\pm13; \pm 23; \pm 9$
crystal system	triclinic	triclinic	monoclinic	monoclinic
space group	$P\bar{1}$	$P\bar{1}$	$C2/c$	$C2/c$
a/Å	6.4000(5)	6.3012(4)	28.0573(7)	11.0004(4)
b/Å	6.5778(6)	6.7360(4)	9.0053(2)	18.6159(7)
c/Å	7.0244(5)	7.3182(5)	21.2997(5)	7.2158(2)
α/deg	81.555(5)	83.084(4)	90.00	90.00
β/deg	69.126(6)	71.846(3)	101.5040(10)	118.241(2)
γ/deg	86.387(6)	86.448(2)	90.00	90.00
V/Å^3	273.29(4)	292.91(3)	5273.6(2)	1301.77(8)
Z	2	2	8	4
D_{calc}/g cm^{-3}	2.201	2.557	2.367	1.690
$F(000)$	178	214	3624	664
μ/mm^{-1}	4.357	10.430	2.687	1.901
max/min transmission	0.8450/0.2883	0.8185/0.2075	0.8774/0.3843	0.9452/0.4816
reflections collected (R_{int})	5307 (0.0329)	6186 (0.0265)	27302 (0.0340)	12268 (0.0351)
independent reflections	1184	1471	5648	1353
obs. reflect. [$I > 2\sigma(I)$]	1093	1366	5531	1250
parameters refined	73	73	405	118
max./min. $\Delta\rho^a$/e Å^{-3}	2.134 /−0.636	0.538/−0.653	1.162/−0.735	0.257/− 0.335
R_1/wR_2 [$I > 2\sigma(I)$]^b	0.0504/0.1605	0.0202/0.0454	0.0433/0.1030	0.0249/0.0638
R_1/wR_2 (all reflect.)^b	0.0527/0.1648	0.0223/0.0461	0.0441/0.1033	0.0276/0.0649
Goodness-of-fit on F^{2c}	1.123	1.076	1.360	1.087
weight. scheme w; a/b^d	0.1323/0.0512	0.0126/0.3592	0.0000/115.7791	0.0351/0.8630

^{a} See footnote a to Table 2. ^{b} See footnote b to Table 2. ^{c} See footnote c to Table 2. ^{d} See footnote d to Table 2. ^{e} Throughout the text the doubled formula of the asymmetric unit was used to have full ligand numbers. ^{f} H atoms on some aqua ligands and crystal water not located but included in formula and formula mass. ^{g} H atoms on partly occupied crystal water not located but included in formula and formula mass.

Table 4. Crystal Data and Structure Refinement for **8**−**10**

compound	8	9	10
Empirical formula	$C_{12}H_{16}Cl_2ZnN_{12}O_8$	$C_{12}H_{16}Cl_2CdN_{12}O_8$	$C_4H_4CuN_4$[e]
M/g mol^{-1}	592.64	639.67	171.65
crystal size/mm	$0.30 \times 0.25 \times 0.10$	$0.12 \times 0.08 \times 0.01$	$0.24 \times 0.15 \times 0.03$
2θ range/deg	3.74−56.28	3.66−63.22	6.28−51.82
h; k; l range	$\pm10; −22, 23; −18, 17$	$−12, 11; −15, 26; −20, 17$	$\pm7; \pm 15; −9, 8$
crystal system	orthorhombic	orthorhombic	monoclinic
space group	$Pnma$	$Pnma$	$P2_1/n$
a/Å	8.0135(3)	8.23350(10)	6.1253(3)
b/Å	17.6580(7)	17.8751(4)	12.9739(9)
c/Å	13.8841(6)	14.2061(3)	7.6245(5)
α/deg	90.00	90.00	90.00
β/deg	90.00	90.00	103.989(2)
γ/deg	90.00	90.00	90.00
V/Å^3	1964.63(14)	2090.78(7)	587.94(6)
Z	4	4	4
D_{calc}/g cm^{-3}	2.004	2.032	1.939
$F(000)$	1200	1272	340
μ/mm^{-1}	1.600	1.373	3.610
max/min transmission	0.8564/0.6453	0.9864/0.8525	0.8994/0.4778
reflections collected (R_{int})	14000 (0.0631)	16400 (0.0599)	4871 (0.0385)
independent reflections	2473	3598	1140
obs. reflect. [$I > 2\sigma(I)$]	1917	2302	1019
parameters refined	172	172	82
max./min. $\Delta\rho^a$/e Å^{-3}	0.848/−0.600	0.752/−0.590	0.424/−0.460
R_1/$wR2$ [$I > 2\sigma(I)$]^b	0.0483/0.1277	0.0358/0.0652	0.0280/0.0611
R_1/wR_2 (all reflect.)^b	0.0639/0.1369	0.0734/0.0757	0.0331/0.0651
Goodness-of-fit on F^{2c}	1.108	1.004	1.080
weight. scheme w; a/b^d	0.0668/2.4355	0.0284/0.0799	0.0222/1.2033

^{a} See footnote a to Table 2. ^{b} See footnote b to Table 2. ^{c} See footnote c to Table 2. ^{d} See footnote d to Table 2. ^{e} Throughout the text the doubled formula of the asymmetric unit was used to have full ligand numbers.

and zinc species compared with the cadmium ones. This also holds for the 3D coordination polymers. Those of copper(I) (**7** and **10**) show a very similar luminescent behavior (Figure

26) and emit around 480 nm under excitation around 280 nm. In the isomorphous zinc and cadmium compounds (**8**

(51) Heller, A. *J. Am. Chem. Soc.* **1966**, *88*, 2058.

(52) Stein, O.; Würzberg, E. *J. Chem. Phys.* **1975**, *62*, 208.
(53) Minaev, B.; Ågren, H. *Chem. Phys.* **2005**, *315*, 215.

and **9**) an emission peaking at 429 nm (**8**) and 403 nm (**9**) was observed when excited around 370 nm. Both of them also show an analogous emission at the same wavelengths if excited at 280 nm, that is, the same excitation wavelength as found in the copper compounds.

Experimental Section

Commercially available solvents, monoformylhydrazine, triethyl orthoformate, ethylenediamine, NH_4SCN, NH_4PF_6, $CuCl_2$, $CuBr_2$, $CuSO_4 \cdot 5H_2O$, $Cu(ClO_4)_2 \cdot 6H_2O$, $ZnCl_2$, $ZnBr_2$, $ZnSO_4$, $Zn(ClO_4)_2 \cdot 6H_2O$, $CdSO_4 \cdot 8/3H_2O$ and $Cd(ClO_4)_2 \cdot 6H_2O$ were used without further purification. **Caution!** *Perchlorate salts of metal complexes are potentially explosive and should be handled with extreme caution and only in very small quantities.* The ligand 1,2-bis(1,2,4-triazol-4-yl)ethane (btre) was prepared according to the method from Bayer.[54] Dried methanol was used for the preparation of the btre ligand. All Cu(I) products were collected under argon atmosphere to avoid oxidative decomposition of the colorless Cu(I) crystals to green colored Cu(II) containing powders in air. Elemental analyses were performed on a VarioEL from Elementaranalysensysteme GmbH. Infrared spectra were recorded in the range $400-4000$ cm^{-1} on a Nicolet Magna 760 Spectrometer using a diamond orbit ATR unit. Thermogravimetric analyses were carried out in a simultaneous thermoanalysis apparatus STA 409C from Netzsch under nitrogen with a heating rate of 10 °C min^{-1} in the range 50 to 600 °C. The filled sample container was conditioned by first applying oil pump vacuum down to 1 bar for 5 min, then flushing with nitrogen.

Powder X-ray diffraction patterns were measured at ambient temperature using a STOE STADI-P with Debye–Scherrer geometry, Mo Kα radiation ($\lambda = 0.7093$ Å), a Ge(111) monochromator and the samples in glass capillaries on a rotating probe head. Simulated powder patterns were based on single-crystal data and calculated using the STOE WinXPOW software package.[55]

Emission spectra were measured on a Perkin-Elmer LS-55, λ_{exc} = $259-285$ nm, split widths (em, ex) 5.0 nm, scan speed 2 nm s^{-1}, solid sample at room temperature.

Syntheses

[Bis{{μ_2-1,2-bis(1,2,4-triazol-4-yl)ethane-$\kappa N1$:$\kappa N1'$}-dichloro-zinc(II)}], [{$ZnCl_2$(μ_2-btre)}$_2$] (1). A mixture of $ZnCl_2$ (136 mg, 1.00 mmol), btre (493 mg, 3.00 mmol), and water (10 mL) was stirred for 30 min at room temperature, transferred to a Teflon-lined stainless-steel autoclave, and heated at 180 °C for 3 d. Then the autoclave was cooled to room temperature at a rate of 2.8 °C h^{-1}. A colorless crystalline product, which was suitable for X-ray single crystal analysis, was filtered off, washed with distilled water, and dried in air (Yield 130 mg, 43% based on Zn). Elemental analysis $C_{12}H_{16}Zn_2N_{12}Cl_4$ (600.91) calcd C 23.99, H 2.68, N 27.97; found: C 23.08, H 2.70, N 27.26%; IR (KBr) 3109(w), 3060(w), 3003(w), 2957(w), 1544(s), 1473(m), 1392(s), 1244(w), 1197(s), 1075(s), 1031(s), 974(w), 871(s), 861(w), 639(s), 488(m), 408(w) cm^{-1}.

[Bis{μ_2-1,2-bis(1,2,4-triazol-4-yl)ethane-$\kappa N1$:$\kappa N1'$}-dibromo-zinc(II)}], [{$ZnBr_2$(μ_2-btre)}$_2$] (2). A mixture of $ZnBr_2$ (235 mg, 1.00 mmol), btre (493 mg, 3.00 mmol), and water (10

mL) was stirred for 30 min at room temperature, transferred to a Teflon-lined stainless-steel autoclave, and heated at 180 °C for 3 d. Then the autoclave was cooled to room temperature at a rate of 2.8 °C h^{-1}. A colorless crystalline product, which was suitable for X-ray single crystal analysis was filtered off, washed with distilled water, and dried in air (Yield 140 mg, 36% based on Zn). Elemental analysis $C_{12}H_{16}Zn_2N_{12}Br_4$ (778.72) calcd C 18.51, H 2.07, N 21.58; found: C 18.22, H 2.09, N 20.92%; IR (KBr) 3102(w), 3060(w), 2998(w), 2951(w), 1543(s), 1470(m), 1391(m), 1363(w), 1241(w), 1194(s), 1072(s), 1028(s), 974(w), 943(w), 868(s), 681(w), 638(s), 485(m), 417(w) cm^{-1}.

catena-[{μ_2-1,2-Bis(1,2,4-triazol-4-yl)ethane-$\kappa N1$:$\kappa N1'$}-bis-(isothiocyanato-κN)-zinc(II)], $^1_\infty$[Zn(NCS)$_2$(μ_2-btre)] (3). A mixture of $ZnSO_4 \cdot 7H_2O$ (164 mg, 0.57 mmol), NH_4SCN (98 mg, 1.30 mmol), btre (233 mg, 1.42 mmol), and water (20 mL) was stirred for 30 min under reflux. The clear colorless solution was left for slow evaporation at room temperature while colorless needles crystals were formed after 1 day, which were suitable for X-ray single crystal analysis. The product was filtered off, washed with distilled water, and dried in air (Yield 140 mg, 71% based on Zn). Elemental analysis $C_8H_8ZnN_8S_2$ (345.71) calcd C 27.79, H 2.33, N 32.41, S 18.55; found: C 27.80, H 2.34, N 32.74, S 18.50%; IR (KBr) 3119(w), 3084(w), 3052(w), 3008(w), 2092(w), 2069(s), 1661(w), 1553(s), 1480(m), 1448(s), 1390(m), 1361(m), 1321(w), 1248(w), 1206(s), 1177(w), 1073(s), 1035(s), 984(m), 955(w), 909(m), 870(w), 834(m), 672(m), 651(s), 623(s), 511(m), 481(m) cm^{-1}.

catena-[{μ_4-1,2-Bis(1,2,4-triazol-4-yl)ethane-$\kappa N1$:$\kappa N2$:$\kappa N1'$:$\kappa N2'$}-dichloro-dicopper(I)], $^2_\infty$[Cu$_2$(μ_2-Cl)$_2$(μ_4-btre)] (4). A mixture of $CuCl_2$ (134 mg, 1.00 mmol), btre (493 mg, 3.00 mmol), and water (10 mL) was stirred for 30 min at room temperature, transferred to a Teflon-lined stainless-steel autoclave, and heated at 180 °C for 3 d. Then the autoclave was cooled to room temperature at a rate of 2.8 °C h^{-1}. A colorless crystalline product, which was suitable for X-ray single crystal analysis, was filtered off, washed with distilled water, dried, and stored under argon (Yield 110 mg, 61% based on Cu). Elemental analysis $C_6H_8Cu_2N_6Cl_2$ (362.19) calcd C 19.90, H 2.23, N 23.20; found: C 20.17, H 2.21, N 23.26%; IR (KBr) 3134(w), 3107(m), 3065(w), 3002(w), 2958(w), 1536(s), 1474(m), 1445(s), 1393(s), 1361(w), 1322(s), 1184(s), 1076(s), 988(s), 871(s), 838(s), 774(m), 683(m), 629(s), 405(w) cm^{-1}.

catena-[{μ_4-1,2-Bis(1,2,4-triazol-4-yl)ethane-$\kappa N1$:$\kappa N2$:$\kappa N1'$:$\kappa N2'$}-dibromo-dicopper(I)], $^2_\infty$[Cu$_2$(μ_2-Br)$_2$(μ_4-btre)] (5). A mixture of $CuBr_2$ (223 mg, 1.00 mmol), btre (493 mg, 3.00 mmol), and water (10 mL) was stirred for 30 min at room temperature, transferred to a Teflon-lined stainless-steel autoclave, and heated at 180 °C for 3 d. Then the autoclave was cooled to room temperature at a rate of 2.8 °C h^{-1}. A colorless crystalline product, which was suitable for X-ray single crystal analysis, was filtered off, washed with distilled water, dried, and stored under argon (Yield 125 mg, 55% based on Cu). Elemental analysis $C_6H_8Cu_2N_6Br_2$ (451.08) calcd C 15.98, H 1.79, N 18.63; found: C 16.37, H 1.66, N 17.84%; IR (KBr) 3130(w),

(54) Bayer, H. O.; Cook, R. S.; von Meyer, W. C. *U. S. Pat.* **1974**, *3*, 821–376.
(55) *STOE WinXPOW*, Version 1.10; STOE & Cie GmbH: Darmstadt, Germany, 2002.

3106(m), 3065(w), 2993(w), 2955(w), 1535(s), 1473(m), 1445(s), 1391(s), 1360(w), 1321(s), 1186(s), 1075(s), 989(s), 863(s), 837(s), 773(s), 681(m), 629(s), 405(w) cm^{-1}.

catena-{Hexaaqua-tris{(μ_4-1,2-bis(1,2,4-triazol-4-yl)ethane-$\kappa N1$:$\kappa N2$:$\kappa N1'$:$\kappa N2'$)}-di(μ_3-hydroxo)-tetra{(μ_3-sulfato-κO,$\kappa O'$,$\kappa O''$)}-hexacadmuim(II)-sulfate-hexahydrate}, $^2_\infty${[Cd$_6$(μ_3-OH)$_2$(μ_3-SO$_4$)$_4$(μ_4-btre)$_3$(H$_2$O)$_6$](SO$_4$)·~6H$_2$O} (6). A mixture of CdSO$_4$·8/3H$_2$O (256 mg, 1.00 mmol), btre (493 mg, 3.00 mmol), and water (10 mL) was stirred for 30 min at room temperature, transferred to a Teflon-lined stainless-steel autoclave, and heated at 180 °C for 3 d. Then the autoclave was cooled to room temperature at a rate of 2.8 °C h^{-1}. A colorless crystalline product, which was suitable for X-ray single crystal analysis, was filtered off, washed with distilled water, and dried in air (Yield 80 mg, 26% based on Cd). Elemental analysis C$_{18}$H$_{50}$Cd$_6$N$_{18}$O$_{34}$S$_5$ (1897.46) calcd C 11.39, H 2.66, N 13.28, S 8.45; found: C 11.45, H 2.66, N 13.24, S 8.48%; IR (KBr) 3094(m), 3039(w), 3010(w), 2974(w), 1679(m), 1525(s), 1454(s), 1384(m), 1270(m), 1223(m), 1222(w), 1187(s), 1112(w), 1062(s), 960(s), 883(s), 783(w), 676(m), 634(s), 419(w) cm^{-1}.

catena-[{(μ_4-1,2-Bis(1,2,4-triazol-4-yl)ethane-$\kappa N1$:$\kappa N2$:$\kappa N1'$:$\kappa N2'$)}-copper(I)] perchlorate hydrate, $^3_\infty${[Cu(μ_4-btre)]ClO$_4$·~0.25H$_2$O} (7). A mixture of Cu(ClO$_4$)$_2$·6H$_2$O (370 mg, 1.00 mmol), btre (493 mg, 3.00 mmol), and water (10 mL) was stirred for 30 min at room temperature, transferred to a Teflon-lined stainless-steel autoclave, and heated at 180 °C for 3 d. Then the autoclave was cooled to room temperature at a rate of 2.8 °C h^{-1}. A colorless crystalline product, which was suitable for X-ray single crystal analysis, was filtered off, washed with distilled water, dried, and stored under argon (Yield 290 mg, 89% based on Cu). Elemental analysis C$_6$H$_8$CuN$_6$O$_4$Cl (327.17) calcd C 22.03, H 2.46, N 25.69; found: C 21.63, H 2.56, N 24.90%; IR (KBr) 3137(w), 2962(w), 1534(m), 1468(m), 1446(w), 1391(m), 1364(w), 1322(w), 1190(s), 1168(m), 1071(s), 988(m), 961(m), 928(w), 857(s), 738(w), 682(w), 620(s), 532(w), 516(w), 485(w), 464(w), 447(w), 409(m) cm^{-1}.

catena-[{(μ_4-1,2-Bis(1,2,4-triazol-4-yl)ethane-$\kappa N1$:$\kappa N2$:$\kappa N1'$:$\kappa N2'$)}-{(μ_2-1,2-bis(1,2,4-triazol-4-yl)ethane-$\kappa N1$:$\kappa N2$)}zinc(II)] diperchlorate, $^3_\infty${[Zn(μ_4-btre)(μ_2-btre)](ClO$_4$)$_2$} (8). A mixture of Zn(ClO$_4$)$_2$·6H$_2$O (372 mg, 1.00 mmol), btre (493 mg, 3.00 mmol), and water (10 mL) was stirred for 30 min at room temperature, transferred to a Teflon-lined stainless-steel autoclave, and heated at 180 °C for 3 d. Then the autoclave was cooled to room temperature at a rate of 2.8 °C h^{-1}. A colorless crystalline product, which was suitable for X-ray single crystal analysis, was filtered off, washed with distilled water, and dried in air (Yield 415 mg, 70% based on Zn). Elemental analysis C$_{12}$H$_{16}$ZnN$_{12}$O$_8$Cl$_2$ (592.64) calcd C 24.32, H 2.72, N 28.36; found: C 24.36, H 2.70, N 27.98%; IR (KBr) 3107(m), 3026(w), 1551(m), 1464(m), 1399(m), 1314(w), 1286(w), 1214(m), 1117(s), 1076(s), 1018(w), 903(m), 864(m), 800(w), 681(m), 618(s), 425(w) cm^{-1}.

catena-[{(μ_4-1,2-Bis(1,2,4-triazol-4-yl)ethane-$\kappa N1$:$\kappa N2$:$\kappa N1'$:$\kappa N2'$)}-{(μ_2-1,2-bis(1,2,4-triazol-4-yl)ethane-$\kappa N1$:$\kappa N2$)}cadmium(II)] diperchlorate, $^3_\infty${[Cd(μ_4-btre)(μ_2-btre)](ClO$_4$)$_2$} (9). A mixture of Cd(ClO$_4$)$_2$·H$_2$O (329 mg, 1.00 mmol), btre (493 mg, 3.00 mmol) and water (10 mL) was stirred for 30 min at room temperature, transferred to a Teflon-lined stainless-steel autoclave, and heated at 180 °C for 3 d. Then the autoclave was cooled to room temperature at a rate of 2.8 °C h^{-1}. A colorless crystalline product, which was suitable for X-ray single crystal analysis, was filtered off, washed with distilled water, and dried in air (Yield 310 mg, 49% based on Cd). Elemental analysis C$_{12}$H$_{16}$CdN$_{12}$O$_8$Cl$_2$ (639.67) calcd C 22.53, H 2.52, N 26.28; found: C 22.49, H 2.48, N 25.78%; IR (KBr) 3105(m), 3024(w), 1554(m), 1463(m), 1395(w), 1313(w), 1281(w), 1218(m), 1117(s), 1073(s), 1027(m), 896(m), 861(m), 795(w), 684(m), 615(s), 463(w), 423(w) cm^{-1}.

catena-[{(μ_4-1,2-Bis(1,2,4-triazol-4-yl)ethane-$\kappa N1$:$\kappa N2$:$\kappa N1'$:$\kappa N2'$)-di-μ_2-cyano-κN:κC-dicopper(I)], $^3_\infty$[Cu$_2$(μ_2-CN)$_2$(μ_4-btre)] (10). A mixture of CuSO$_4$·5H$_2$O (250 mg, 1.00 mmol), btre (493 mg, 3.00 mmol), and water (10 mL) was stirred for 30 min at room temperature, transferred to a Teflon-lined stainless-steel autoclave, and heated at 180 °C for 3 d. Then the autoclave was cooled to room temperature at a rate of 2.8 °C h^{-1}. A colorless crystalline product, which was suitable for X-ray single crystal analysis, was filtered off, washed with distilled water, dried, and stored under argon (Yield 135 mg, 79% based on Cu). Elemental analysis C$_8$H$_8$Cu$_2$N$_8$ (343.30) calcd C 27.99, H 2.35, N 32.64; found: C 27.68, H 2.36, N 33.06%; IR (KBr) 3120(m), 3003(w), 2959(w), 2094(s), 1539(s), 1453(m), 1394(s), 1362(w), 1324(s), 1191(s), 1075(s), 1001(m), 863(s), 840(w), 776(s), 679(m), 632(s), 439(w) cm^{-1}.

Solid-State NMR

All spectra were recorded using 2.5 mm rotors on a Bruker Avance 500 solid-state NMR spectrometer (11.7 T) operating at Lamor frequencies of 125.78 MMz for ^{13}C. RF pulses were applied at a transverse B1 field of 125 kHz corresponding to a $\pi/2$ pulse width of 2 μs. ^{13}C {^{1}H} CPMAS experiments were performed under magic angle spinning at 20 KHz and 30 kHz with bearing gas at ambient temperature. Cross polarization was achieved using a ramp[56] with typically 1024 steps applied to the proton channel ranging from 80 to 100% and a contact time of 2 ms. In all ^{13}C experiments, TPPM dipolar decoupling[57] was employed. ^{13}C spectra were referenced to the methyne resonance of alanine (51 ppm).

Fluorescence Spectroscopy

Photoluminescence analyses for the fluorescing powders of compounds **2**, **4**, **5**, **7**, **8**, **9**, and **10** were performed at room temperature on a Perkin-Elmer LS55 fluorescence

(56) (a) Metz, G.; Ziliox, M.; Smith, S. O. *Solid State Nucl. Magn. Reson.* **1996**, *7*, 155–160. (b) Metz, G.; Wu, X.; Smith, S. O. *J. Magn. Reson. A* **1994**, *110*, 219–227. (c) Metz, G.; Wu, X.; Smith, S. O. *Chem. Phys. Lett.* **1994**, *173*, 461–465.
(57) Bennett, A. E.; Rienstra, C. M.; Auger, M.; Lakshmi, K. V.; Griffin, R. G. *J. Chem. Phys.* **1995**, *103*, 6951–6958.

spectrometer equipped with a Xe discharge lamp (equivalent to 20 kW for 8 μs duration) and a gated photomultiplier with modified S5 response.

X-ray Crystallography

Suitable single crystals were carefully selected under a polarizing microscope. *Data Collection:* Bruker AXS with APEXII CCD area-detector, Mo Kα radiation ($\lambda = 0.71073$ Å), graphite monochromator, double-pass method ω-scan, Data collection and cell refinement with APEX2,[58] respectively, cell refinement and data reduction with SAINT,[58] experimental absorption correction with SADABS.[59] *Structure Analysis and Refinement*: The structure was solved by direct methods (SHELXS-97);[60] refinement was done by full-matrix least-squares on $F2$ using the SHELXL-97 program suite.[60] All non-hydrogen positions were refined with anisotropic temperature factors. Hydrogen atoms on carbon were positioned geometrically (C−H = 0.98 Å for CH$_2$, 0.94 Å for aromatic CH) and refined using a riding model (AFIX 23, 43, respectively), with $U_{iso}(H) = 1.2U_{eq}(C)$. In the structure of **6** the hydrogen atom on the hydroxo O atom was positioned geometrically (O−H = 0.99 Å) and refined using a riding model (AFIX 13), with $U_{iso}(H) = 1.2U_{eq}(O)$. Hydrogen atoms on the aqua ligand O2 and the half-occupied crystal water O7 were found but had to be kept fixed in subsequent refinement. Hydrogen atoms on the other aqua ligands O1 and O3 and the other crystal water O atoms O5 and half-occupied O6, O35, and O36 could not be found. The non-coordinated sulfate group around S3 is disordered near an inversion center. It also resides on a split position with the half-occupied crystal water O atoms O35 and O36. In the structure of **7** the Cl atom of the perchlorate group sits on a special position (2-fold rotation axis, Wyckoff notation 4e, 1/2 y 1/4). The four oxygen atoms of the perchlorate groups are disordered over 8 positions. Some residual electron density is assigned to a partially occupied

water oxygen atom. The occupation of this crystal water adds up to 1 crystal water per unit cell. No hydrogen atoms could be found or refined for this partially occupied O atom. The structure of **10** could also be refined to identical *R*-values in the monoclinic space group $P2_1/c$ with the cell constants $a = 6.1253(3)$, $b = 12.9739(9)$, $c = 8.5483(4)$ Å, $\beta = 120.062(3)°$, $V = 587.94(6)$ Å^3. Graphics were obtained with DIAMOND.[61] Details of the supramolecular C−H···N/X (X = Cl, Br, S) and π-π interaction were calculated by the program PLATON.[62] π-Stacking interactions can be viewed as medium to weak if they exhibit rather long centroid-centroid distances (Cg···Cg > 4.0 Å) together with large slip angles (β, γ > 30°) and vertical displacements (d > 2.0 Å). In comparison, strong π-stackings show rather short centroid-centroid contacts (<3.8 Å), small slip angles (β, γ < 25°) and vertical displacements (d < 1.5 Å) which translate into a sizable overlap of the aromatic planes.[39,63,64] Crystal data and details on the structure refinement are given in Table 2−4. The structural data has been deposited with the Cambridge Crystallographic Data Center (CCDC-numbers. 710669 to 710678 for **1**−**10**, respectively).

Supporting Information Available: Crystal reactivity of **7**, **8**, or **9** with NH$_4$PF$_6$/H$_2$O, thermogravimetric analyses, X-ray powder diffractograms, tables of intermolecular interactions, tables of selected bond distances and angles, additional pictures of networks, CPMAS ^{13}C, and ^{1}H NMR spectra (26 pages). This material is available free of charge via the Internet at http://pubs.acs.org.

IC802069K

(58) *APEX2 (Version 2.1−0) Data Collection Program for the CCD Area-Detector System; SAINT, Data Reduction and Frame Integration Program for the CCD Area-Detector System*; Bruker Analytical X-ray Systems: Madison, WI, 2006.

(59) Sheldrick, G. *Program SADABS: Area-detector absorption correction*; University of Göttingen: Göttingen, Germany, 1996.

(60) Sheldrick, G. M. *SHELXS-97, SHELXL-97, Programs for Crystal Structure Analysis*; University of Göttingen: Göttingen, Germany, 1997.

(61) Brandenburg, K. *Diamond (Version 3.1e), Crystal and Molecular Structure Visualization, Crystal Impact*; K. Brandenburg & H. Putz Gbr: Bonn, Germany, 2007.

(62) (a) Spek, A. L. *J. Appl. Crystallogr.* **2003**, *36*, 7–13. (b) Spek, A. L. *PLATON - A Multipurpose Crystallographic Tool*; Utrecht University: Utrecht, The Netherlands, 2008; Windows implementation: L. J. Farrugia, University of Glasgow, Scotland, Version 40608 (2008).

(63) (a) Monfared, H. H.; Kalantari, Z.; Kamyabi, M.-A.; Janiak, C. *Z. Anorg. Allg. Chem.* **2007**, *633*, 1945–1948. (b) Wu, B.; Huang, X.; Xia, Y.; Yang, X.-J.; Janiak, C. *CrystEngComm* **2007**, *9*, 676–685. (c) Wisser, B.; Janiak, C. *Acta Crystallogr.* **2007**, *E63*, o2871–2872. (d) Dorn, T.; Janiak, C.; Abu-Shandi, K. *CrystEngComm* **2005**, *7*, 633.

(64) Yang, X.-J.; Drepper, F.; Wu, B.; Sun, W.-H.; Haehnel, W.; Janiak, C. *Dalton Trans.* **2005**, 256–267; and supplementary material therein.